ORNL-2860
Particle Accelerators and
High-Voltage Machines

THE ADMITTANCE AND TRANSFER FUNCTIONS OF SOLID CORE ELECTROMAGNETS

N. F. Ziegler

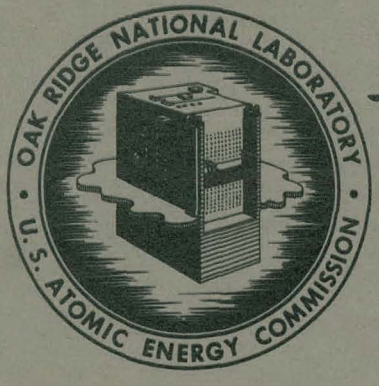

OAK RIDGE NATIONAL LABORATORY
operated by
UNION CARBIDE CORPORATION
for the
U.S. ATOMIC ENERGY COMMISSION

DISCLAIMER

Printed in USA. Price $1.75. Available from the
Office of Technical Services
Department of Commerce
Washington 25, D.C.

ORNL-2860

Contract No. W-7405-eng-26

ELECTRONUCLEAR RESEARCH DIVISION

THE ADMITTANCE AND TRANSFER FUNCTIONS OF SOLID CORE ELECTROMAGNETS

N. F. Ziegler

Submitted as a thesis to The Graduate Council of The University of Tennessee in partial fulfillment of the requirements for the degree of Master of Science.

DATE ISSUED

JAN 18 1960

OAK RIDGE NATIONAL LABORATORY
operated by
UNION CARBIDE CORPORATION
for the
U.S. ATOMIC ENERGY COMMISSION

THIS PAGE

WAS INTENTIONALLY

LEFT BLANK

TABLE OF CONTENTS

LIST OF FIGURES

CHAPTER I

INTRODUCTION

The problem posed for this thesis was the determination of the admittance and transfer functions of large, solid-core electromagnets. The effects of eddy currents and hysteresis were considered in deriving the functions. Specifically, the study was concerned with the type of magnet employed in nuclear physics research which requires very precise regulation (0.1% to 0.001%) of the magnetic field.

Although a number of papers have been written on eddy currents and hysteresis in transformers, inductors, and rotating machinery, the results are not directly applicable to a magnet which is a part of a closed-loop system. Most of the papers have been concerned with core losses in electrical equipment. Therefore, the purpose of this paper is to consolidate and simplify the previous results for the special case of a magnet in which the variations in flux density are very small. Eddy currents external of the iron (in coil support and cooling plates) were also considered in deriving the admittance and transfer functions.

There are, of course, other factors besides eddy currents which influence the dynamics of an electromagnet. One of these has been termed a "delay-line" effect by Dr. Bob Smith of the University of California since, in some cases, the leakage inductance of the magnet winding combines with the winding capacitance to produce a "transport lag." According to Dr. Smith this effect occurs primarily in high-voltage, low-current magnets which employ a large number of turns in

the winding. This paper, however, will be limited to the study of eddy current and hysteresis effects.

This study originated during the design of an analyzing magnet regulator for the ORNL 63-inch cyclotron. The admittance of this particular magnet was modified considerably by external eddy currents in the coil support plates (see Figure 18). Although consideration of only the external eddy currents seemed to provide quite accurate analytical results, it was known that internal eddy currents and hysteresis could also affect the admittance. Therefore, this study was initiated to determine the magnitude of these effects.

The results of this paper should be of considerable importance to the designer of magnet control systems since eddy currents can modify greatly the magnet admittance from that usually assumed. Since this function is always "inside" the regulator loop, it has a large influence on the design of the regulating system. In Chapter IV it will be demonstrated that neglect of eddy current coupling can result in an unstable regulator. The magnet transfer function is "outside" the loop of a current regulator and does not affect the stability of such a system. If eddy currents exist, however, this function assumes the characteristics of a rather peculiar low-pass filter and thus aids in removing high-frequency variations from the magnetic field.

In developing the admittance and transfer functions the frequency response method has been employed rather than the Laplace Transform since the results are somewhat simpler although less general. In Chapter II the functions are derived for various cross-sectional shapes of

iron. Chapter III presents some experimental results from a cylindrical core test magnet and from the analyzing magnet. In Chapter IV the possible effects of eddy currents on the regulating system are considered.

Most of the symbols employed in the analysis are more or less standard in the field of electrical engineering. Where necessary, symbols are defined in the text.

The rationalized MKS system of units is used throughout the paper.

CHAPTER II

DEVELOPMENT OF MAGNET ADMITTANCE AND TRANSFER FUNCTIONS

It has been common practice to assume that the admittance of a magnet winding was

$$Y_m = \frac{1}{R_m} \frac{1}{1 + j\omega T_m} .$$

However, as will be shown, this is a very poor approximation for solid core magnets having low leakage inductance.

In deriving the admittance and transfer functions in this chapter, the following conditions have been assumed:

1. The incremental permeability of the magnet core is constant for small variations in flux density (B).
2. The hysteresis loop for the iron core is elliptical in shape for small variations in $B^{(1)}$.
3. Flux in the magnet air gap is uniformly distributed, and there is no fringing flux.

In order to determine the effects of eddy current coupling and hysteresis, consider the equivalent circuit shown in Figure 1 in which the subscript m refers to the magnet winding, and subscript s refers to the short circuit winding or "shorted-turn." L_1 and L_2 are the leakage

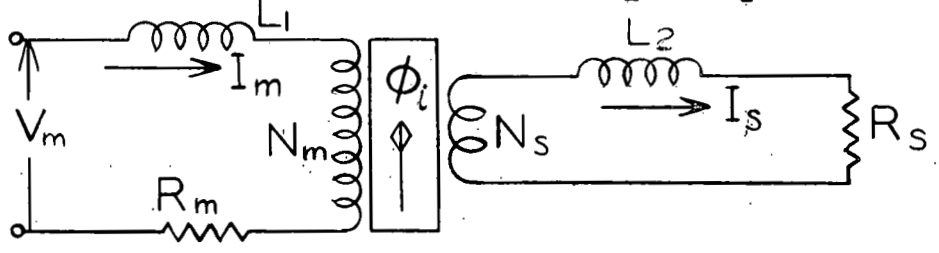

Figure 1. Equivalent Circuit of a Magnet

inductances of the magnet winding and shorted turn, respectively, and ϕ_i is the flux linking both N_m and N_s.

The equations describing this circuit may be written as

$$\begin{aligned} V_m &= I_m(R_m + j\omega L_1) + j\omega N_m \phi_i \\ 0 &= -j\omega N_s \phi_i + I_s(R_s + j\omega L_2) \\ \phi_i &= (1/\mathcal{R})(N_m I_m - N_s I_s) \end{aligned} \qquad (1)$$

(where $\mathcal{R}$ is the reluctance of the magnetic circuit) or by eliminating ϕ_i,

$$\begin{aligned} V_m &= I_m\left[R_m + j\omega(L_1 + N_m^2/\mathcal{R})\right] - j\omega I_s N_m N_s/\mathcal{R} \\ 0 &= -j\omega I_m N_m N_s/\mathcal{R} + I_s\left[R_s + j\omega(L_2 + N_s^2/\mathcal{R})\right] \end{aligned}$$

$$\text{Let } \mathcal{R} = \mathcal{R}_o/Q$$

$$L_m = N_m^2/\mathcal{R}_o \qquad (2)$$

$$L_s = N_s^2/\mathcal{R}_o$$

$$\text{and } k = L_1/L_m = L_2/L_s,$$

where $\mathcal{R}_o$ is the zero frequency reluctance and Q is a function which, as will be shown, involves the effect of internal eddy currents and hysteresis.

Then

$$Y_m = \frac{I_m}{V_m} = \frac{R_s + j\omega L_s(k + Q)}{\left[R_m + j\omega L_m(k + Q)\right]\left[R_s + j\omega L_s(k + Q)\right] - (j\omega)^2 L_m L_s Q^2}$$

$$= \frac{1}{R_m} \frac{1 + j\omega T_s(k + Q)}{\left[1 + j\omega T_m(k + Q)\right]\left[1 + j\omega T_s(k + Q)\right] - (j\omega)^2 T_m T_s Q^2} \qquad (3)$$

If Q is set equal to one, Equation 3 will be recognized as the input

admittance of a transformer with a shorted secondary, i.e.,

$$Y_m = \frac{1}{R_m} \frac{1 + j\omega T_s(1 + k)}{1 + j\omega(T_m + T_s)(1 + k) + (j\omega)^2 T_m T_s k(2 + k)}$$

and if $k << 0.5$

$$Y_m \approx \frac{1}{R_m} \frac{1 + j\omega T_s}{\left[1 + j\omega(T_m + T_s)\right]\left[1 + j\omega \frac{2kT_m T_s}{T_m + T_s}\right]} . \qquad (4)$$

It will be shown that setting $Q = 1$ is equivalent to neglecting internal eddy currents; therefore, Equation 4 is the input admittance of a magnet considering only external eddy currents in the coil support and cooling plates. The normalized admittance of the 63-inch cyclotron analyzing magnet (shown in Figure 18) was found to be in very good agreement with Equation 4.

The transfer function of a magnet may also be obtained from Equation 1 with the following result:

$$G = \frac{B_g}{I_m} = \frac{\phi_g}{A_g I_m} = \frac{N_m}{A_g \mathcal{R}_o} Q \frac{1 + j\omega k T_s}{1 + j\omega T_s(k + Q)}$$

where B_g, ϕ_g, and A_g are, respectively, the air gap flux density, total flux and cross-sectional area. Under the assumed conditions $\phi_g = \phi_i$. If internal eddy currents and hysteresis are again neglected ($Q = 1$),

$$G = \frac{N_m}{A_g \mathcal{R}_o} \frac{1 + j\omega k T_s}{1 + j\omega T_s(1 + k)} . \qquad (6)$$

Thus, the external eddy currents in a shorted turn attenuate the effect of variations in I_m for $\omega T_s >> 1/(1 + k)$.

In order to determine the effect of internal eddy currents and hysteresis on the dynamics of a magnet consider the magnetic circuit

in Figure 2. It is assumed that the pole tips are covered with a very thin sheet of the hypothetical material having infinite permeability and zero conductivity[2]. This assumption permits the non-uniform flux in the core to have a uniform distribution in the air gap. If a rigorous solution is attempted without the above assumption, the solution involves a series of Bessel functions, and even if the resulting boundary value problem could be solved, it would be of doubtful practical value due to its complexity.

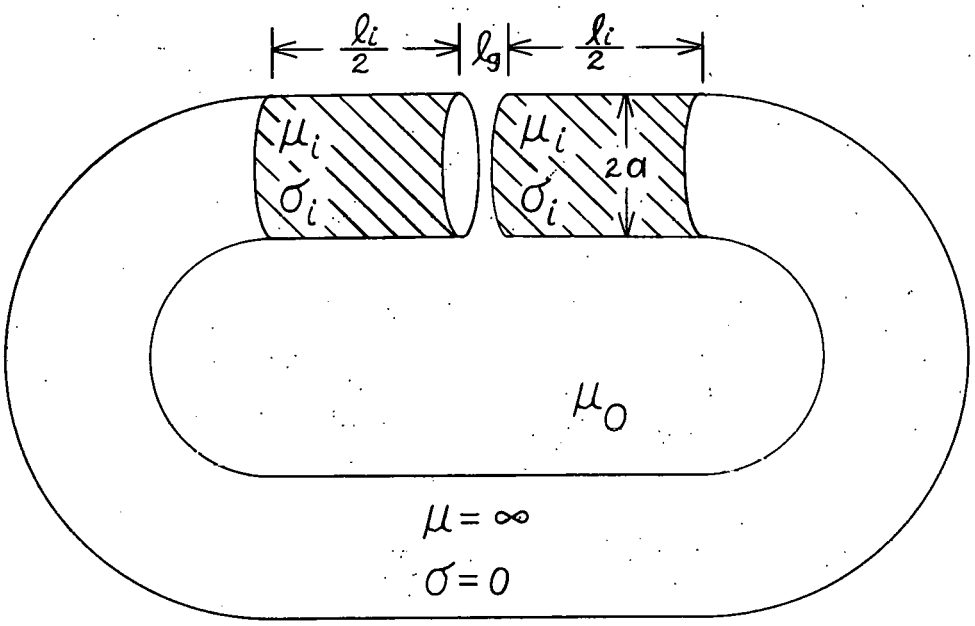

Figure 2. A Cylindrical Core Magnet.

Under the above conditions it can be shown that the axial flux density in the cylindrical iron poles is given by[3].

$$B_i = B_a \frac{J_o(\gamma r)}{J_o(\gamma a)} , \qquad (7)$$

where B_i = flux density at radius r, B_a = flux density at the surface of the cylindrical pole, $\gamma = \sqrt{-j\omega\sigma_i\mu_i}$, and $J_o(\gamma r)$ is the zero-th order Bessel function of the first kind. In the air gap

$$B_g = \frac{1}{\pi a^2} \int_o^a 2\pi r B_i dr$$

$$= \frac{2}{a^2} \frac{B_a}{J_o(\gamma a)} \int_o^a r\, J_o(\gamma r) dr$$

$$= \frac{2B_a}{\gamma a} \frac{J_1(\gamma a)}{J_o(\gamma a)} .$$

At r = a,

$$\int_o^{\ell_g/2} (B_g/\mu_o) dz + \ell_{g/2} \int^{\frac{\ell_g + \ell_i}{2}} \frac{B_i}{\mu_i} dz = F/2,$$

where F = mmf. acting on the magnetic circuit,

or

$$\frac{2B_a \ell_g}{\mu_o \gamma a} \frac{J_1(\gamma a)}{J_o(\gamma a)} + B_a \frac{\ell_i}{\mu_i} = F,$$

and $$B_a = \frac{\mu_i \gamma a J_o(\gamma a)}{2\mu_r \ell_g J_1(\gamma a) + \gamma a \ell_i J_o(\gamma a)} F,$$

where $$\mu_r = \frac{\mu_i}{\mu_o} .$$

Therefore $$\phi_g = \phi_i = \pi a^2 B_g$$

$$= \frac{2\pi a^2 \mu_i J_1(\gamma a)}{2\mu_r \ell_g J_1(\gamma a) + \ell_i \gamma a J_o(\gamma a)} F,$$

and $$\mathcal{R} = \frac{\ell_g}{\pi a^2 \mu_o} \left[1 + \frac{\ell_i}{\mu_r \ell_g} \frac{\gamma a}{2} \frac{J_o(\gamma a)}{J_1(\gamma a)} \right] .$$

The zero-frequency reluctance of the magnetic circuit is

$$\mathcal{R}_o = \frac{\ell_g}{\pi a^2 \mu_o}\left[1 + \frac{\ell_i}{\mu_r \ell_g}\right].$$

Therefore, from Equation 2

$$Q = \frac{\mathcal{R}_o}{\mathcal{R}} = \frac{1 + \dfrac{\ell_i}{\mu_r \ell_g}}{1 + \dfrac{\ell_i}{\mu_r \ell_g}\dfrac{\gamma a}{2}\dfrac{J_o(\gamma a)}{J_1(\gamma a)}} \tag{8}$$

for a cylindrical core.

As stated previously, assuming $Q = 1$ is equivalent to neglecting internal eddy currents since $\gamma = 0$ for $\omega = 0$ and

$$\lim_{\gamma a \to 0}\left[\frac{\gamma a}{2}\frac{J_o(\gamma a)}{J_1(\gamma a)}\right] \longrightarrow 1 \text{ and } Q \longrightarrow 1.$$

If hysteresis is neglected the Bessel functions involved in Equation 8 will be recognized as the ber and bei functions; however, for the purposes of this paper it will be advantageous to employ the polar form(3)

$$J_o\left(\beta\angle 135°\right) = M_o \angle \Psi_o$$

$$J_1\left(\beta\angle 135°\right) = M_1 \angle \Psi_1$$

where $\beta = a\sqrt{\omega\sigma_i\mu_i}$

Then $$\frac{\gamma a}{2}\frac{J_o(\gamma a)}{J_1(\gamma a)} = \frac{\beta}{2}\frac{M_o}{M_1}\angle 135° + \Psi_o - \Psi_1 = N_o \angle \theta_o .$$

A graph of N_o and θ_o is shown in Figure 3 plotted as a function of ω/ω_e where

$$\omega_e = \frac{4}{a^2\sigma_i\mu_i} \tag{9}$$

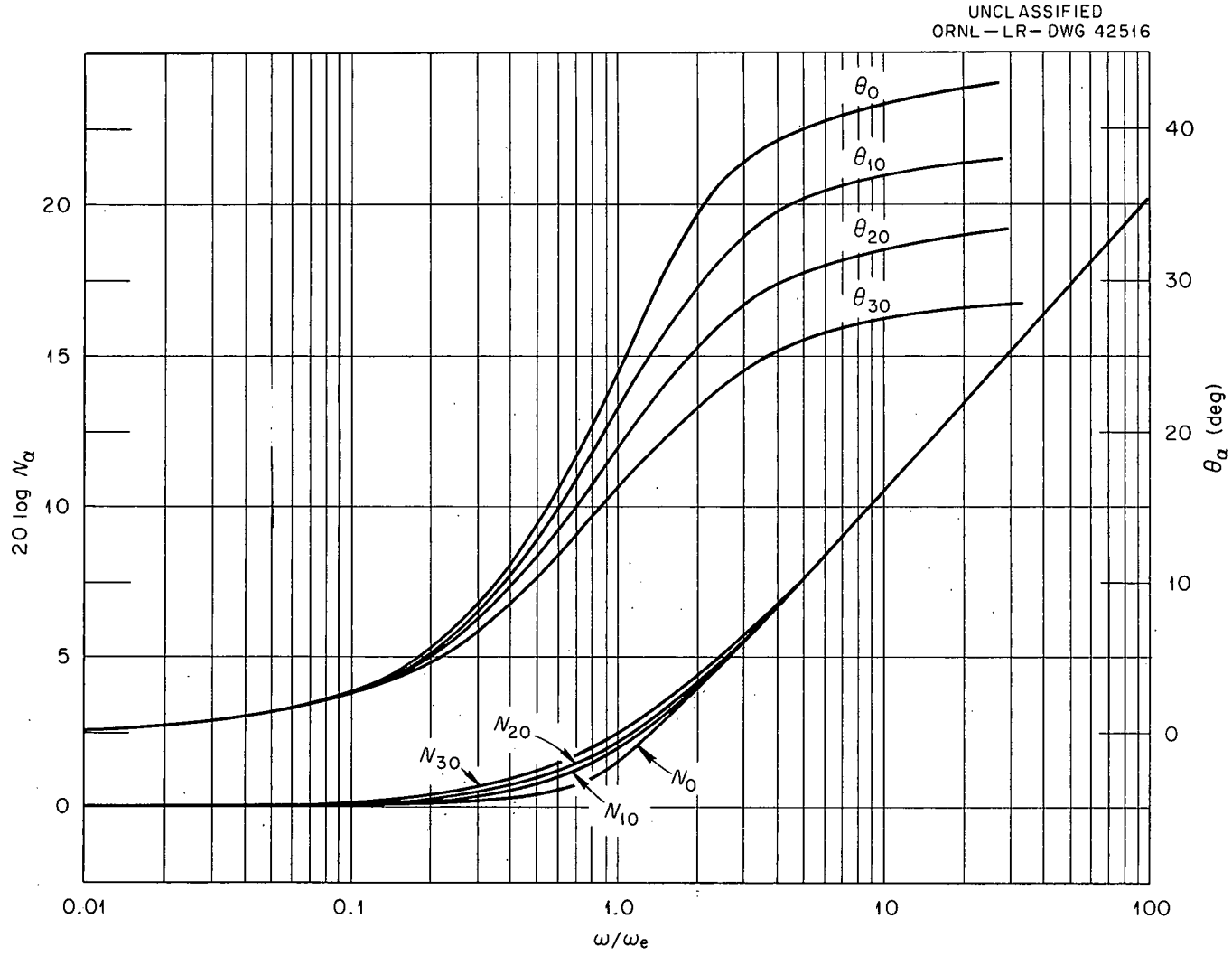

Figure 3. Graph of N_α and Θ_α.

$$\text{or} \quad \omega/\omega_e = (\beta/2)^2 \ .$$

The general shape of the N_o and θ_o curves implies that a good approximation to the function $N_o \ \underline{/\theta_o}$ would be

$$N_o \ \underline{/\theta_o} \approx \sqrt{1 + j\omega/\omega_e}$$

This approximation has been checked in the range $0.0025 \leq \omega/\omega_e \leq 100$ and is indeed a very good approximation for engineering purposes. The maximum error in magnitude is approximately three percent and in phase is about three degrees, both occuring at $\omega/\omega_e \approx 3$.

With $N_o \ \underline{/\theta_o} \approx \sqrt{1 + j\omega/\omega_e}$, Equation 8 becomes

$$Q \approx \frac{1 + \ell_i/\mu_r \ell_g}{1 + (\ell_i/\mu_r \ell_g)\sqrt{1 + j\omega/\omega_e}} \ . \qquad (10)$$

For most large magnets $\ell_i/\mu_r \ell_g << 1$ since $\ell_i/\mu_r \ell_g$ is the ratio of core reluctance to air gap reluctance, and this ratio must be small if the magnet is to be efficient. Under this condition then

$$Q \approx \frac{1}{1 + (\ell_i/\mu_r \ell_g)\sqrt{1 + j\omega/\omega_e}} \ .$$

For internal eddy currents to affect, appreciably, the magnet dynamics, Q must be considerably less than one. A rough approximation of the frequency at which internal eddy currents become important may then be obtained by assuming

$$(\ell_i/\mu_r \ell_g)\left|\sqrt{1 + j\omega_E/\omega_e}\right| = 1$$

where ω_E is the approximate frequency. If $\ell_i/\mu_r \ell_g << 1$ then ω_E/ω_e must be much greater than one for the above to be true. Then

$$(\ell_i/\mu_r \ell_g)\sqrt{\omega_E/\omega_e} \approx 1$$

$$\text{or} \qquad \omega_E \approx (\mu_r \ell_g/\ell_i)^2 \omega_e. \qquad (11)$$

It is of some importance to note that ω_E is directly proportional to μ_r, provided, of course, that $\ell_i/\mu_r \ell_g << 1$, while ω_e is inversely proportional to μ_r.

It is not possible, in general, to simplify Equations 3 and 5 if both internal and external eddy currents are considered. However, for the cylindrical core magnet with no external eddy currents ($T_s = 0$) and $\ell_i/\mu_r \ell_g << 1$ the following asymptotic expressions can be derived.

$$\left.\begin{aligned} Y_m &\approx \frac{1}{R_m}\frac{1}{1 + j\omega T_m(1+k)} \\ G_m &\approx \frac{N_m}{A_g \mathcal{R}_o} \end{aligned}\right\} \text{ for } \omega << \omega_E$$

$$\left.\begin{aligned} Y_m &\approx \frac{1}{R_m}\frac{1}{1 + j\omega T_m(k + 1/\sqrt{j\omega/\omega_E})} \\ G_m &\approx \frac{N_m}{A_g \mathcal{R}_o}\frac{1}{\sqrt{j\omega/\omega_E}} \end{aligned}\right\} \text{ for } \omega >> \omega_E \text{ and } |Q| >> k,$$

and

$$\left.\begin{aligned} Y_m &\approx \frac{1}{R_m}\frac{1}{1 + j\omega k T_m} \\ G_m &\approx \frac{N_m}{A_g \mathcal{R}_o}\frac{1}{\sqrt{j\omega/\omega_E}} \end{aligned}\right\} \text{ for } |Q| << k.$$

It should be emphasized that the above results are very "rough" approximations. However, since the computations involved in more exact expressions are quite lengthy, they should prove useful.

To illustrate, in a more accurate manner, the effect of internal eddy currents, consider the following example for a cylindrical core magnet.

Let $T_m = 1.9$ sec.

$T_s = 0$

$k = 0.05$

$a = 0.5$m.

$\ell_i / \ell_g = 50$

$\mu_r = 1000$

$\sigma_i = 10^7$ mho/m.

Then $\omega_e = 1/785$

and

$$Y_m \approx \frac{1}{R_m} \frac{1}{1 + j1.9\omega \left(0.05 + \frac{1}{1 + 0.05\sqrt{1 + j785\omega}} \right)} .$$

A normalized Bode plot of the above function is shown in Figure 4 along with a plot of the function $1/(1 + j2\omega)$ which is the normalized admittance if eddy currents are neglected.

The transfer function for the above example is

$$G \approx \frac{N_m}{A_g \mathcal{R}_o} \frac{1}{1 + 0.05\sqrt{1 + j785\omega}} .$$

A normalized plot of this function is shown in Figure 5. If eddy currents are neglected, G is of course a constant. It is evident from Figures 4 and 5 that the internal eddy currents have a considerable effect on the magnet dynamics for this assumed case. To illustrate the effect of a "shorted turn", assume $T_s = 0.48$ seconds in the previous example.

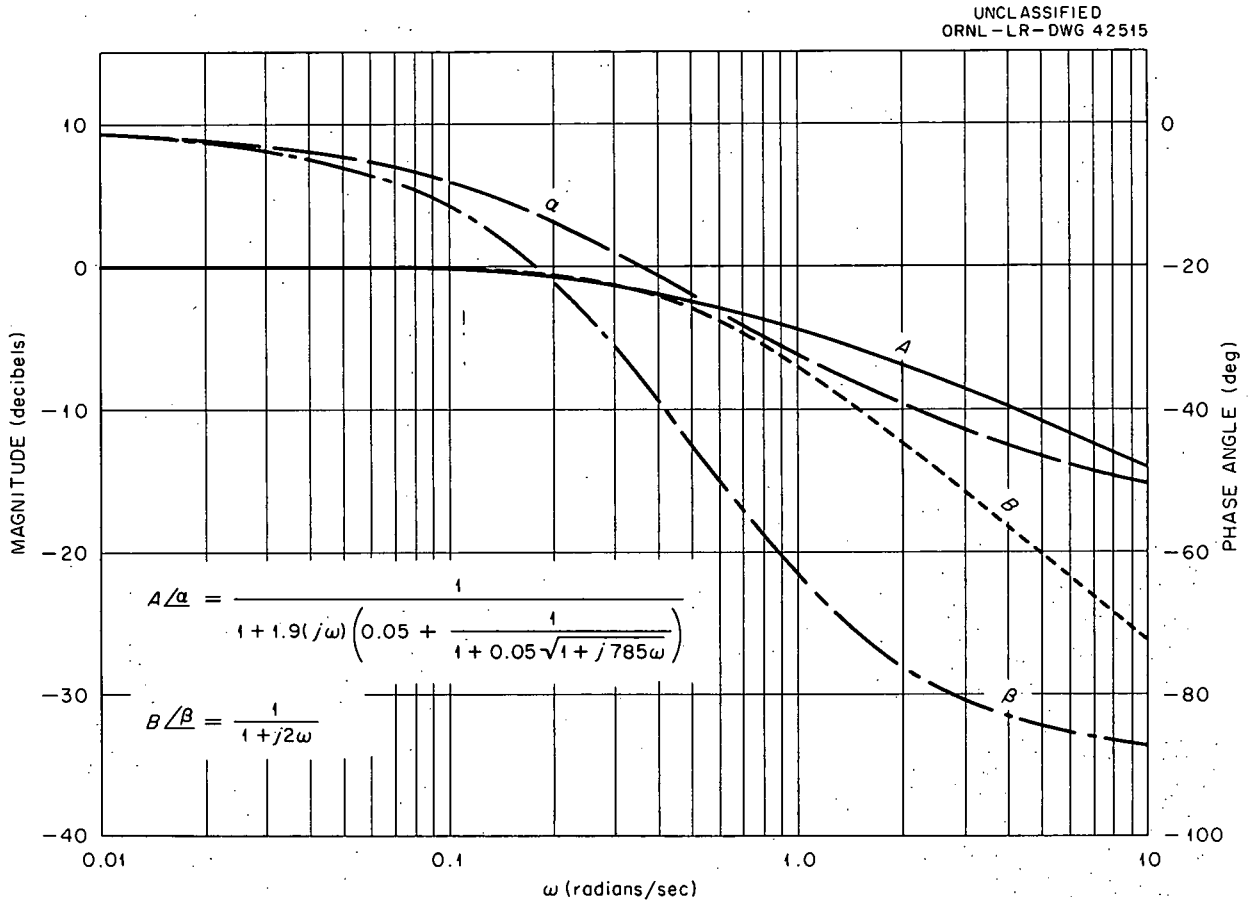

Figure 4. Normalized Magnet Admittance for an Assumed Case.

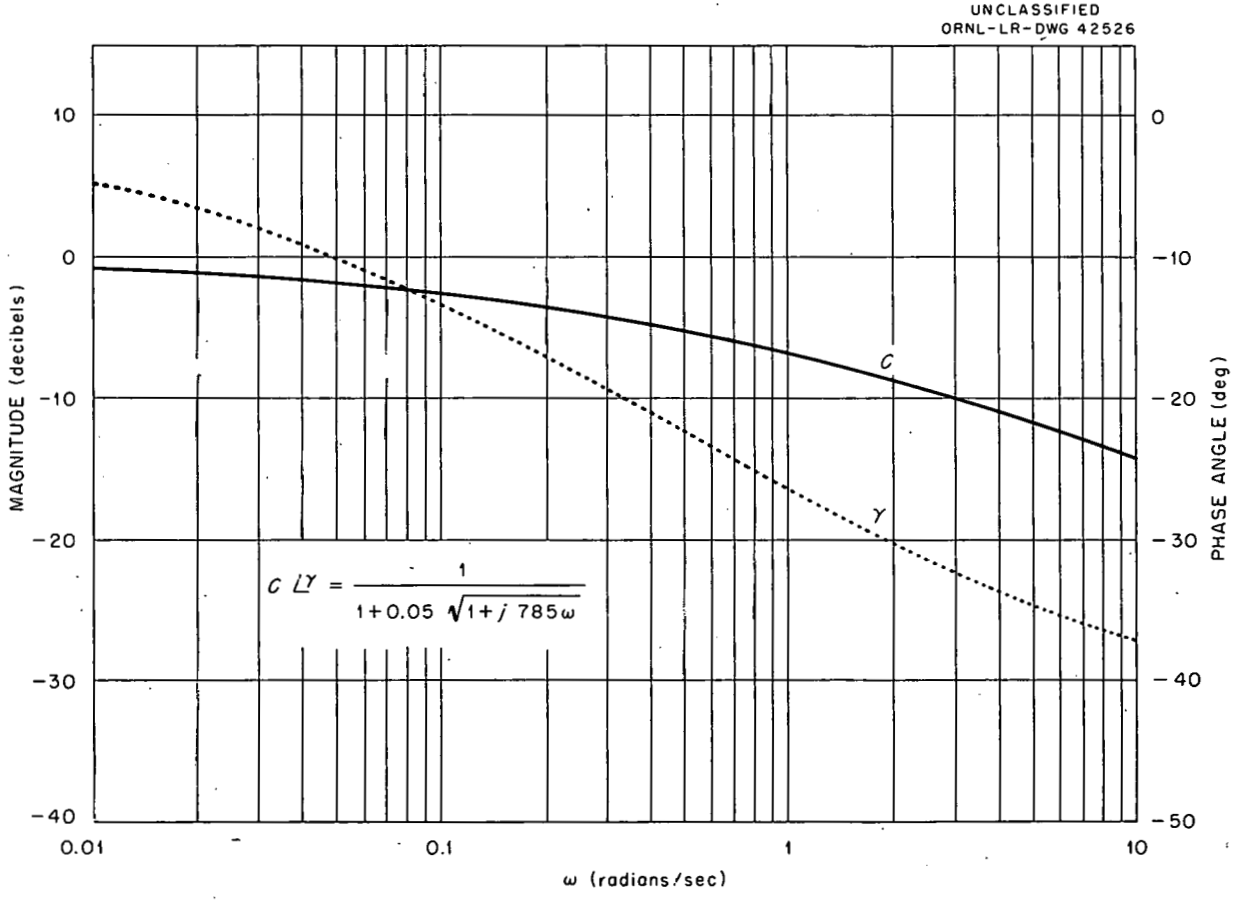

Figure 5. Normalized Magnet Transfer Function for Assumed Case.

Then

$$Y_m = \frac{1}{R_m} \frac{1 + j\omega(0.48)(0.05 + Q)}{\left[1 + j\omega(0.48)(0.05 + Q)\right]\left[1 + j\omega(1.9)(0.05 + Q)\right] - (j\omega)^2 (0.912)Q},$$

$$G = \frac{N_m}{A_g \mathcal{R}_o} \frac{1 + j\omega(0.024)}{1 + j\omega(0.48)(0.05 + Q)} Q,$$

where

$$Q \approx \frac{1}{1 + 0.05\sqrt{1 + j785\omega}}.$$

The normalized values of Y_m and G are plotted in Figures 6 and 7, respectively. The external eddy currents in the "shorted turn" have a rather small effect on the magnet admittance in this particular case. The transfer function is affected to a greater extent, but the effect is still rather minor. However, it should not be inferred that this is always true.

To consider the effect of hysteresis on the magnet admittance and transfer functions, the hysteresis loop must, in some manner, be replaced by an equivalent linear effect, since hysteresis produces non-linearities even on an incremental basis. Several authors have suggested that the hysteresis loop may be assumed elliptical in shape[1][4][5], in which case $B = \mu_o \mu_r' \exp(-j\alpha)H$. Then the relative permeability as used in the previous development becomes

$$\mu_r = \mu_r' \exp(-j\alpha).$$

In the admittance and transfer functions which have been developed, the complex permeability would modify only the inductances and the function Q. For the cylindrical core magnet with complex permeability

$$\frac{L_m}{N_m^2} = \frac{L_s}{N_s^2} = \frac{\pi a^2 \mu_o}{\ell_g + (\ell_i/\mu_r')\exp(j\alpha)},$$

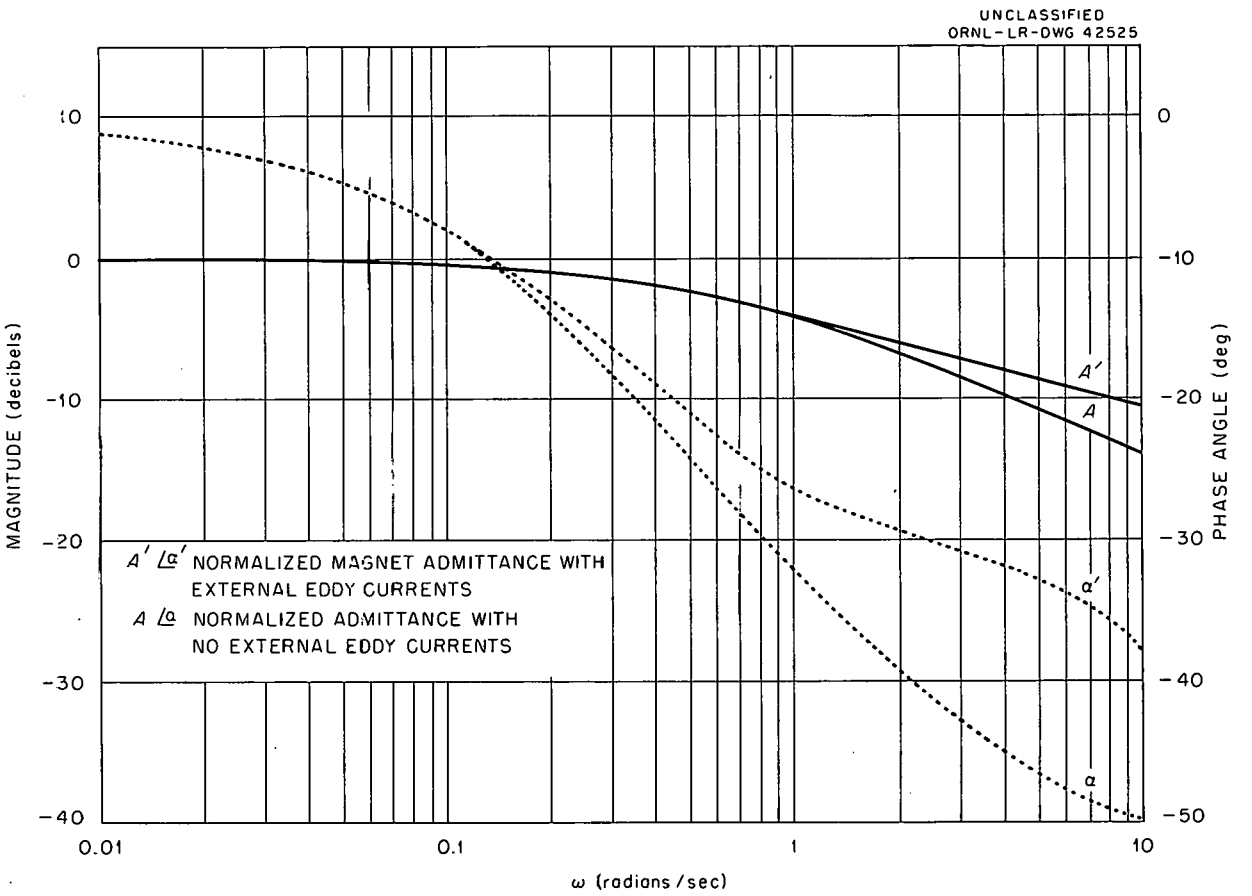

Figure 6. The Effect of External Eddy Currents on Magnet Admittance.

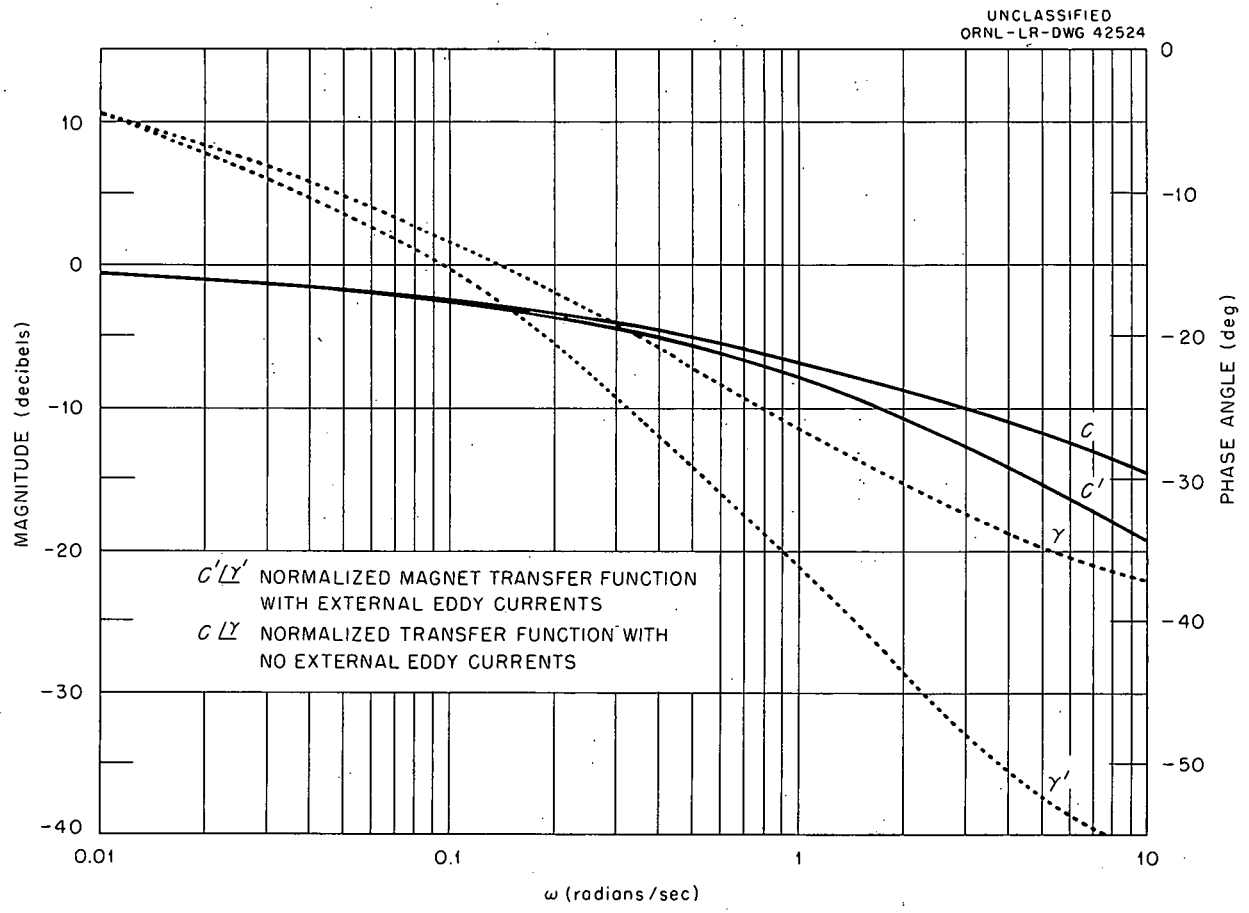

Figure 7. The Effect of External Eddy Currents on a Magnet Transfer Function.

and

$$Q = \frac{1 + (\ell_i/\mu_r' \ell_g)\exp(j\alpha)}{1 + (\ell_i/\mu_r' \ell_g)\exp(j\alpha)N_\alpha/\theta_\alpha} \quad .$$

Also

$$N_\alpha/\theta_\alpha = \frac{\gamma' a}{2} \frac{J_o(\gamma' a)}{J_1(\gamma' a)}$$

where

$$\gamma' = \sqrt{-j \exp(-j\alpha)\omega\sigma_i\mu_o\mu_r'} \quad .$$

If it is again assumed that $(\ell_i/\mu_r' \ell_g) << 1$, then it is obvious that the effect of hysteresis on the inductances is very small and may be neglected. In fact, if the assumption is invalidated by saturation of the iron, the effect on L_m and L_s will still be very small since the angle α would also decrease with saturation. Therefore, in the remainder of the development it will be assumed that L_m and L_s are unaffected by hysteresis. For $(\ell_i/\mu_r' \ell_g) << 1$

$$Q \approx \frac{1}{1 + (\ell_i/\mu_r' \ell_g)N_\alpha \underline{/\theta_\alpha + \alpha}} \quad .$$

Graphs of N_α and θ_α are shown in Figure 3 for $\alpha = 0°$, $10°$, $20°$, and $30°$. It appears from these curves that complex permeability has little effect on N_α except in the region $0.1 < \omega/\omega_e < 10$. It can also be shown that

$$\lim_{\omega/\omega_e \to 0} N_\alpha \to 1$$

and

$$\lim_{\omega/\omega_e \to \infty} N_\alpha \to \sqrt{\omega/\omega_e} \quad .$$

The angle θ_α is affected to a much greater extent however. In fact, it can be shown that

$$\lim_{\omega/\omega_e \to \infty} \theta_\alpha \to (45° - \alpha/2).$$

Therefore $\lim_{\omega/\omega_e \to \infty} (\theta_\alpha + \alpha) \to (45° + \alpha/2)$.

It is rather difficult to state, in general, the effect of hysteresis on magnet admittance and transfer functions. However, for the case in which $T_s = 0$ and $\sqrt{\omega_e} \approx 1/T_m$, hysteresis causes the rate of attenuation and the phase of Y_m to be less than that of a magnet without hysteresis. The transfer function, for the same conditions, will attenuate more rapidly and the phase angle will be greater than that of a magnet without hysteresis. For both the admittance and the transfer function, hysteresis affects primarily the phase angle; the effect on attenuation is rather minor. Since the angle, α, is small for "soft" magnetic materials, it appears that hysteresis effects are negligible, in most cases, as compared to eddy current effects.

Thus far only cylindrical core magnets have been considered. In practice, of course, large magnets are seldom, if ever, constructed with this configuration throughout. Although the magnet poles may be cylindrical, the yoke, or return path, is normally rectangular in cross-section. In many cases the pole also is non-cylindrical. Analyzing magnets in particular have very peculiar pole cross-sections such as triangular, semi-circular, rectangular, or combinations of these. For any cross-section other than circular, an exact solution for the flux distribution would be extremely difficult. It should be possible to approximate the effect of eddy currents in odd cross-section, however, by applying the solutions for the infinite sheet and semi-infinite solid. For an infinite sheet of magnetic material it can be shown that[4]

$$B_i = B_a \frac{\cosh(-j\gamma x)}{\cosh(-j\gamma t/2)} \qquad (12)$$

where t = thickness of the sheet,

x = distance from center of sheet perpendicular to the surface,

$\gamma = \sqrt{-j\omega\sigma_i\mu_i}$,

B_a = flux density at surface of sheet,

B_i = flux density at x.

To apply Equation 12 to a rectangular yoke it is apparent that the width, d, of the yoke should be much greater than the thickness, t, as shown in Figure 8. Since this is not always true, a new width d' may be defined as follows[5]:

$$\begin{cases} d' = d + t - 2\delta & \text{for } \delta < t/2 \\ d' = d & \text{for } \delta > t/2 \end{cases}$$

where $\delta = \dfrac{1}{\sqrt{\omega\sigma_i\mu_i}}$.

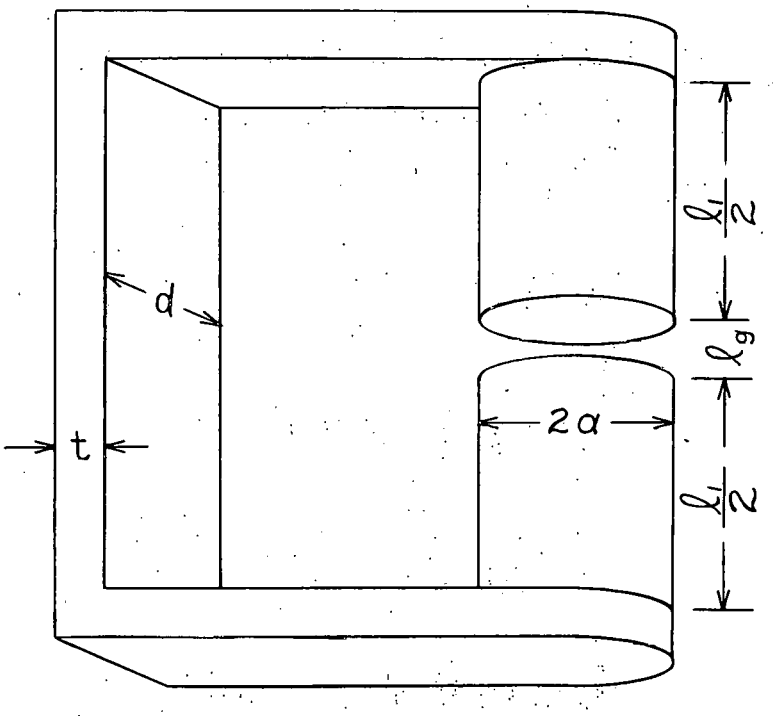

Figure 8. "C-Type" Magnet Core.

The above definition considers in an approximate manner the flux which flows along the edges of the rectangular sheet. With this definition the average flux density in the rectangular yoke of Figure 8 is

$$B_o \approx \frac{d'}{d} \int_{-t/2}^{t/2} B_i dx$$

$$\approx \frac{d'}{d} \frac{B_a}{(-j\gamma t/2)} \tanh(-j\gamma t/2). \qquad (13)$$

The reluctance of a length ℓ_i of the rectangular yoke is then

$$\mathcal{R} = F/\phi = \frac{H_s \ell_i}{B_o A_y} = \frac{B_a \ell_i}{\mu_i B_o A_y}$$

$$= \frac{\ell_i}{\mu_i A_y} (S/\eta) \qquad (14)$$

where H_s = magnetic field intensity at the iron surface,

A_y = td, the cross-sectional area of the yoke,

and $S/\eta = d/d' \dfrac{-j\gamma t/2}{\tanh(-j\gamma t/2)}$.

The function S/η is plotted in Figure 9 for three t/d ratios. It can be shown that

$$S/\eta = \begin{cases} \dfrac{\sqrt{j\omega/\omega_e}}{\tanh\sqrt{j\omega/\omega_e}} & \text{for } \omega/\omega_e \leq 1 \\ \dfrac{1}{1 + (t/d)(1 - 1/\sqrt{\omega/\omega_e})} \dfrac{\sqrt{j\omega/\omega_e}}{\tanh\sqrt{j\omega/\omega_e}} & \text{for } \omega/\omega_e > 1, \end{cases} \qquad (15)$$

where $\omega_e = \dfrac{4}{\sigma_i \mu_i t^2}$.

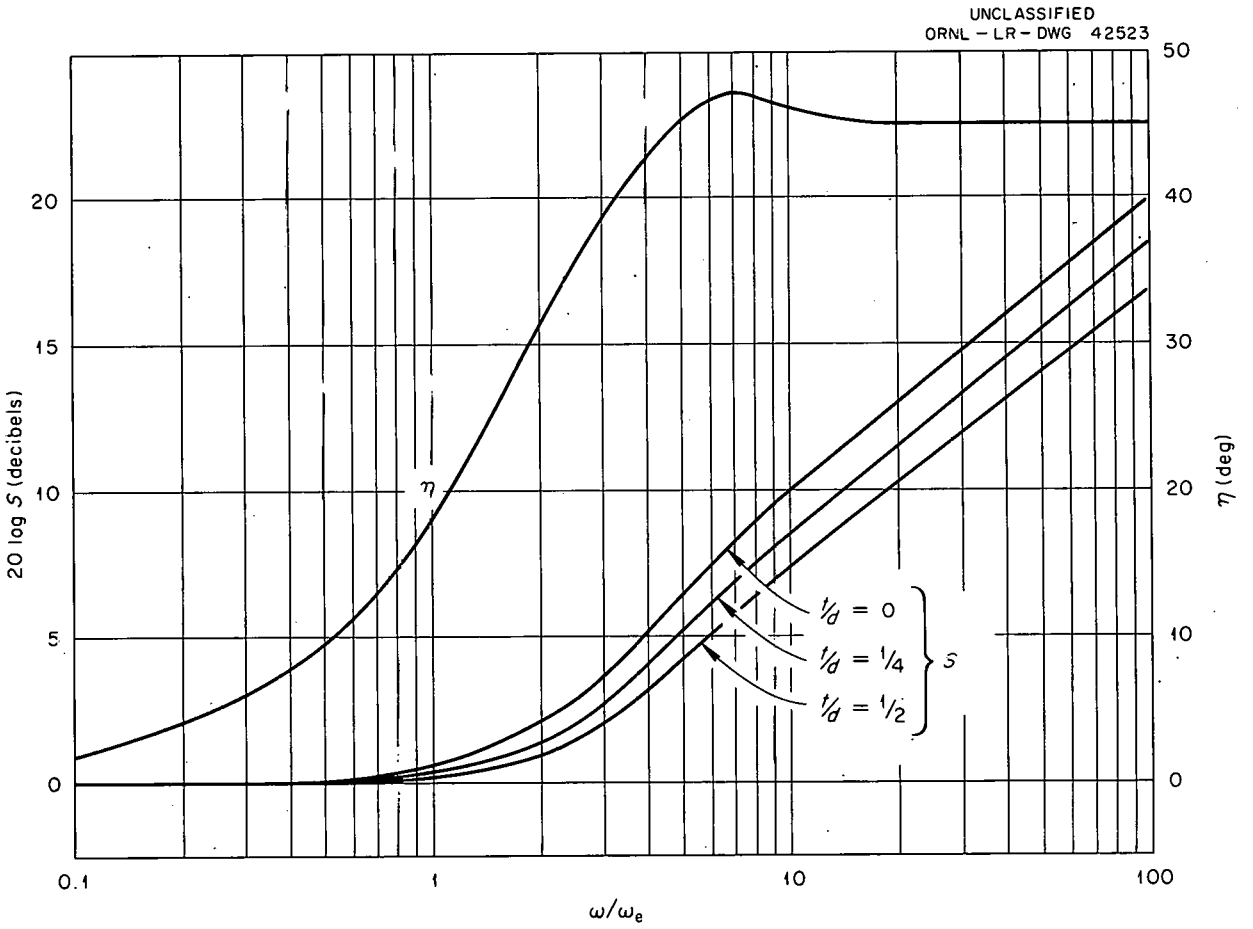

Figure 9. Graph of S and η.

From Equation 15 and Figure 9 it is apparent that for $\sqrt{\omega/\omega_e} >> 1$

$$S/\eta \approx \frac{\sqrt{\omega/\omega_e}}{1 + t/d} \; /45° \quad .$$

As defined above, ω_e for the rectangular yoke will, in most cases, be somewhat larger than ω_e for a cylindrical yoke of the same cross-sectional area.

By employing Equation 14 it is possible to determine, approximately, the effect of internal eddy currents on cyclotron magnets, which usually have a rectangular yoke and cylindrical poles. Two types of construction are common for these magnets - the "C-type" core and the "H-type" core. Consider first the "C-type" configuration shown in Figure 8 for which it is assumed that the iron in the yoke and poles is of the same type, the flux in the gap is uniformly distributed, and that the length of the rectangular yoke is ℓ_2. The effect of the corners and of the circular-to-rectangular transition will be neglected. The total reluctance of the magnetic circuit is then

$$\mathcal{R}_T = \frac{\ell_g}{\mu_o A_g} + \frac{\ell_1}{\mu_i A_p} N_o \; /\theta_o + \frac{\ell_2}{\mu_i A_y} \; S/\eta \quad ,$$

and the zero-frequency reluctance is

$$\mathcal{R}_o = \frac{\ell_g}{\mu_o A_g} + \frac{\ell_1}{\mu_i A_p} + \frac{\ell_2}{\mu_i A_y} \quad ,$$

giving

$$Q = \frac{1 + \frac{\ell_1}{\mu_r \ell_g} \frac{A_g}{A_p} \frac{\ell_2}{\mu_r \ell_g} \frac{A_g}{A_y}}{1 + \frac{\ell_1}{\mu_r \ell_g} \frac{A_g}{A_p} \; N_o/\theta_o + \frac{\ell_2}{\mu_r \ell_g} \frac{A_g}{A_y} S/\eta} \quad . \qquad (16)$$

Under the assumption that the flux is uniformly distributed in the air gap, the air gap area, A_g, is equal to the pole area, A_p. However, it is advantageous to include the ratio, A_g/A_p, in Equation 16 since this permits the fringing flux, which is always present in an actual case, to be considered in an approximate manner.

For the "H-type" yoke, Q may be obtained directly from Equation 16 since there are, in effect, two "C-type" yokes in parallel. Then

$$Q = \frac{1 + \frac{\ell_1}{\mu_r \ell_g}\frac{A_g}{A_p} + \frac{\ell_2}{\mu_r \ell_g}\frac{A_g}{2A_y}}{1 + \frac{\ell_1}{\mu_r \ell_g}\frac{A_g}{A_p}\ N_o/\underline{\theta_o} + \frac{\ell_2}{\mu_r \ell_g}\frac{A_g}{2A_y}\ S/\underline{\eta}} \quad . \tag{17}$$

It is possible to determine an ω_E for the rectangular yoke also, if it is again assumed that ω_E is the frequency at which

$$\frac{\mathcal{R}_{oy}}{\mathcal{R}_g} S = 1$$

where $\mathcal{R}_{oy}$ = zero-frequency reluctance of rectangular yoke. If $\mathcal{R}_{oy}/\mathcal{R}_g << 1$, then $S >> 1$ at ω_E

$$\text{and } S \approx \frac{\sqrt{\omega_E/\omega_e}}{1 + t/d}$$

$$\text{or } \frac{\mathcal{R}_{oy}}{\mathcal{R}_g}\frac{\sqrt{\omega_E/\omega_e}}{1 + t/d} \approx 1.$$

$$\text{Then } \omega_E \approx \left(\frac{1 + t/d}{\mathcal{R}_{oy}/\mathcal{R}_g}\right)^2 \omega_e \quad . \tag{18}$$

For iron-cross-sections which are neither circular nor rectangular it is necessary to resort to further approximations to determine the effect

of internal eddy currents. Since the internal eddy currents tend to force the time-varying flux toward the surface of the iron for any pole or yoke shape, it should be possible to employ the solution for flux distribution in a semi-infinite magnet in approximating the effect of eddy currents. For the semi-infinite magnet occupying the entire lower half space

$$B_i = B_a \exp(j\gamma x),$$

where B_a = flux density at the iron surface

B_i = flux density x meters from iron surface

$\gamma = \sqrt{-j\omega\sigma_i\mu_i}$

x = distance into the iron perpendicular to iron surface.

Then the total time-varying flux in a section of the solid y meters wide is

$$\begin{aligned}\phi &= y \int_0^\infty B_i dx \\ &= (y/-j\gamma)B_a \\ &= y\delta B_a \exp(-j\pi/4),\end{aligned}$$

where $\delta = \dfrac{1}{\sqrt{\omega\sigma_i\mu_i}}$.

And, the reluctance of a section y meters wide and ℓ_i meters long is

$$\begin{aligned}\mathcal{R} &= \frac{B_a \ell_i}{\phi \mu_i} \\ &= \frac{\ell_i}{\mu_i} \frac{1}{y\delta} \angle 45^\circ .\end{aligned} \qquad (19)$$

The use of Equation 19 in estimating the effect of eddy currents in odd shaped poles may best be illustrated by a simple example. Consider that two poles such as the one sketched in Figure 10 are employed with a rectangular "C-type" yoke to form an analyzing magnet. Then the

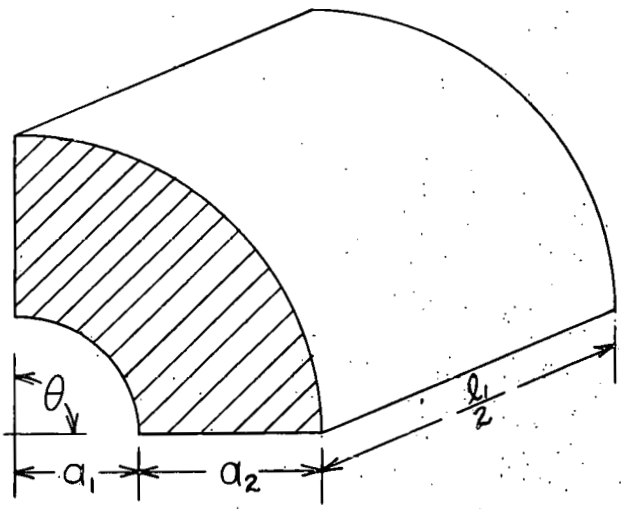

Figure 10. Magnet Pole of Odd Cross-Section.

reluctance of the poles is

$$\mathcal{R}_p \approx \frac{\ell_1}{\mu_i \delta} \frac{1/45^\circ}{\left[2a_1\theta + (2 + \theta)a_2 - 4\delta\right]}$$

$$\text{for } \delta << \frac{a_2}{2} \text{ and } \frac{\theta a_1}{2} .$$

The zero-frequency reluctance of the poles is

$$\mathcal{R}_{op} = \frac{\ell_1}{\mu_i} \frac{2}{\theta a_2(a_2 + 2a_1)} = \frac{\ell_1}{\mu_i A_p} ,$$

and for the magnet

$$Q \approx \frac{1 + \frac{\ell_1}{\mu_r \ell_g}\frac{A_g}{A_p} + \frac{\ell_2}{\mu_r \ell_g}\frac{A_g}{A_y}}{1 + \frac{\ell_1}{\mu_r \ell_g}\frac{A_g \angle 45^\circ}{\delta\left[2a_1\theta + (2+\theta)a_2 - 4\delta\right]} + \frac{\ell_2}{\mu_r \ell_g}\frac{A_g}{A_y} \; S\angle\eta} ,$$

if $\delta << \frac{a_2}{2}$ and $\frac{\theta a_1}{2}$.

CHAPTER III

EXPERIMENTAL RESULTS

To check the theory developed in the preceding chapter a small magnet was constructed having, approximately, the dimensions shown in Figure 11. The core was formed from a one-inch round bar of 1018 steel

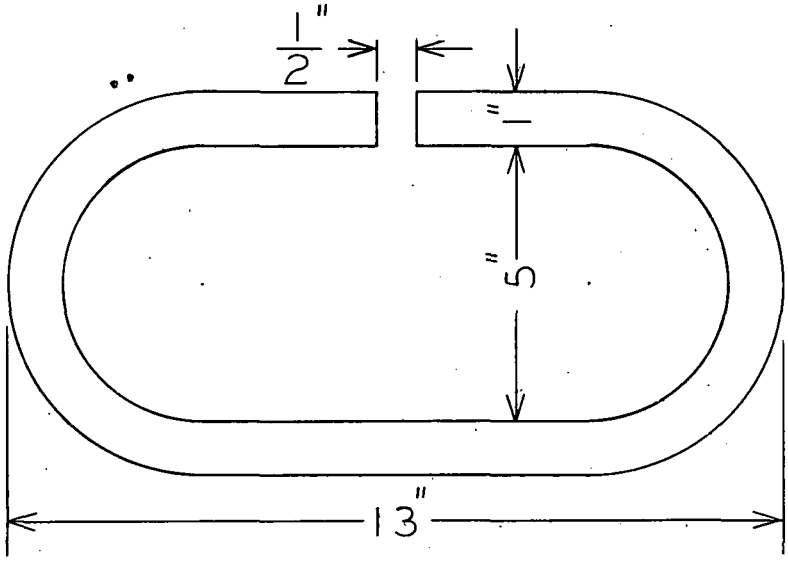

Figure 11. Test Magnet Core.

and annealed after forming. The exciting winding consisted of eighteen 100-turn coils wound of #18 copper wire. The coils were distributed uniformly around the core to minimize the leakage inductance. A 600-turn "pick-up" coil was also placed on the core in order to measure the magnet transfer function.

The one-half inch air gap was a rather unfortunate choice since the large gap-to-pole diameter ratio resulted in a large amount of "fringing flux" which in turn complicated, and reduced the accuracy of, the calculations. The relatively large air gap was chosen in order that the coils

could be easily installed and to provide access for a rotating-coil flux meter.

A magnetization curve for the test magnet is shown in Figure 12. This is a graph of the flux density in the center of the air gap and pole as a function of magnet winding current. In this case it should be termed an "air-gap flux-density curve" since the flux density in the iron is considerably greater than that shown on the curve. This fact is illustrated by Figure 13 which is a plot of flux density versus radius, or distance from the pole center. It is obvious from this curve that the "fringing flux" was quite large for the test magnet. To compensate for this fact an equivalent air gap area was calculated by determining, approximately, the total flux crossing a surface in the center of the air gap and dividing this flux by the flux density at the pole center. For a field having circular symmetry

$$\phi = 2\pi \int_0^\infty rB(r)dr;$$

therefore, if B(r) in Figure 13 is multiplied by r and the resulting curve is integrated graphically, the total flux in the iron is obtained approximately. The curve rB(r) is also shown in Figure 13. Since measurements out to $r = \infty$ are somewhat impractical the area under the curve, rB(r), out to r = 2 was obtained with a planimeter and the remaining area estimated by assuming that the slope of the curve was constant for $r \geq 2$ and $rB(r) \geq 0$. From this calculation the equivalent cross-sectional area of the air gap was computed to be 3.38 square inches and the flux density in the iron

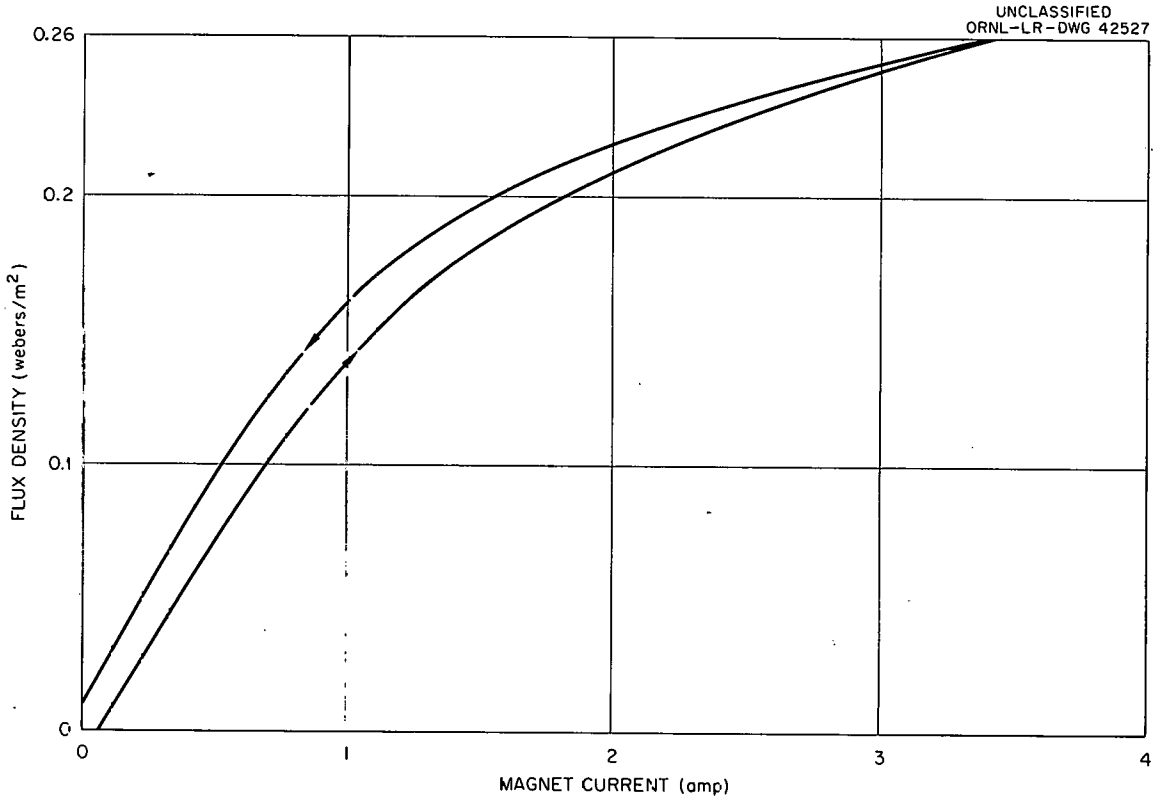

Figure 12. Magnetization Curve of Test Magnet.

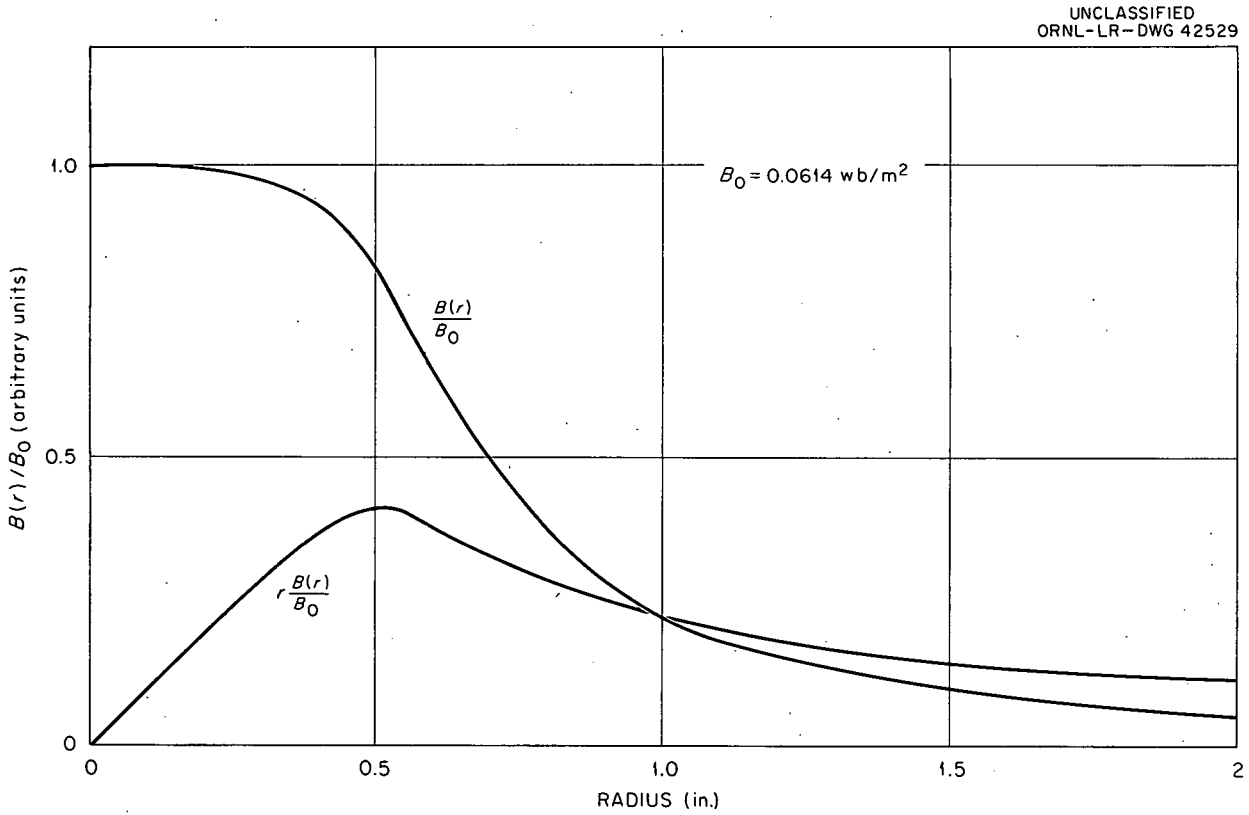

Figure 13. Radial Variation of Flux Density in Test Magnet Air Gap.

$$B_i = \frac{A_g}{A_i} B_o = \frac{3.38}{\pi/4} B_o$$

$$= 4.25\ B_o$$

where A_g = equivalent air gap area,

B_o = air gap flux density at r = 0.

Of course the flux distribution around the air gap is not truly symmetrical for the test magnet due to the return yoke, but the approximation should be reasonably accurate.

To calculate L_m, μ_r, and α it was necessary to obtain a minor hysteresis loop for the magnet. Such a loop is shown in Figure 14. Since the maximum slope of the magnetization curve in Figure 12 occurs in the vicinity of $I_m = 0.4$ amp, all measurements and calculations were made for a quiescent magnet current of 0.4 ampere. The values of the incremental quantities calculated from the minor hysteresis loop are as follows:

$$L_m = 0.352 \text{ hy}$$

$$\mu_r = 274$$

$$\alpha = 10^\circ \quad .$$

The d-c resistance of the magnet winding was determined to be 3.92 ohms giving

$$T_m = \frac{L_m}{R_m} \approx 0.09 \text{ sec.}$$

The conductivity of 1018 steel is given as $0.7(10^7)$ mhos per meter resulting in

$$\omega_e = \frac{4}{a^2 \sigma_i \mu_i} \approx 10.3 \text{ rad/sec},$$

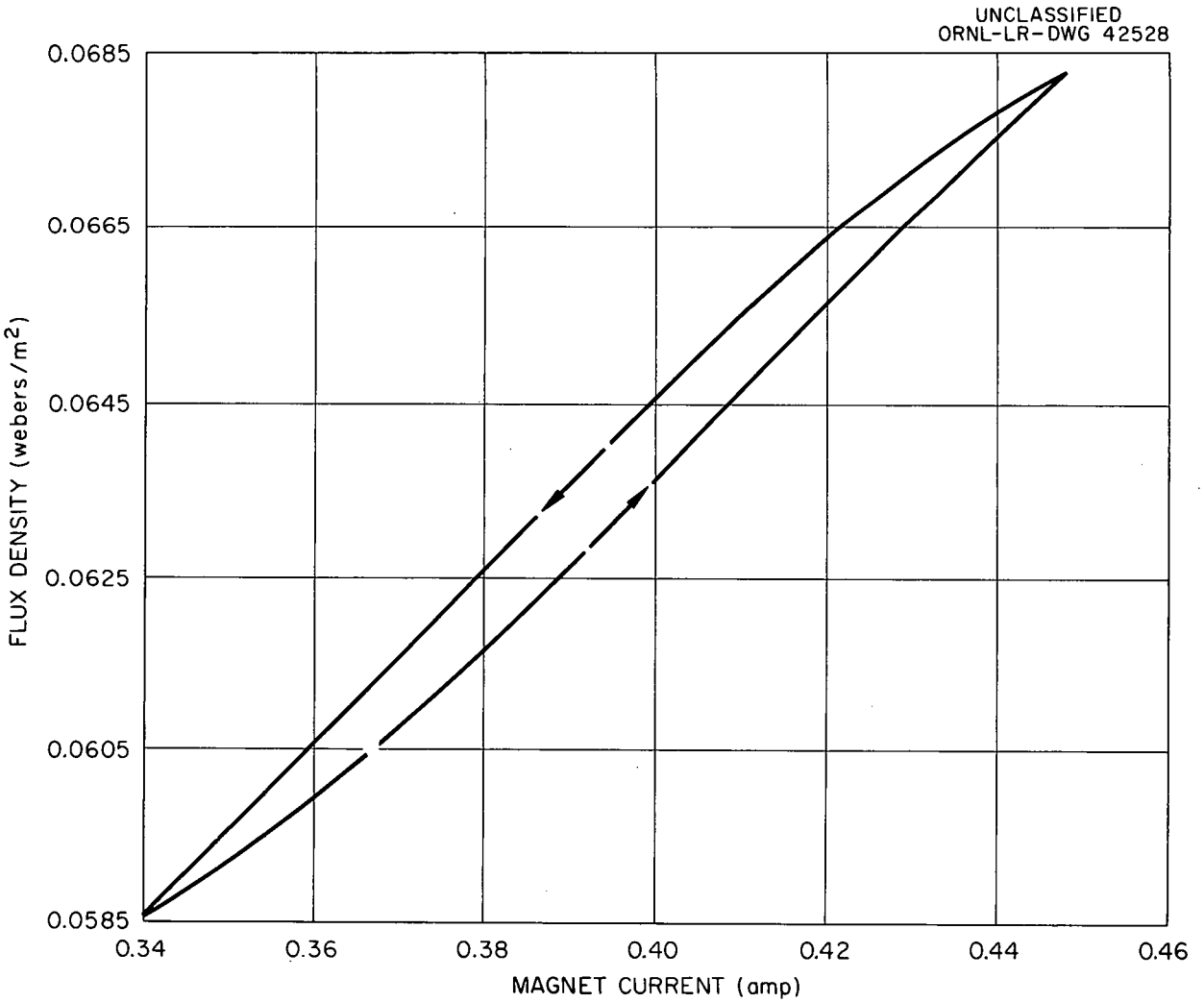

Figure 14. Minor Hysteresis Loop for Test Magnet.

and the ratio of the zero-frequency reluctance of the iron to the air gap reluctance is

$$\frac{\ell_i}{\mu_r \ell_g} \frac{A_g}{A_i} \approx 0.973.$$

Since the above ratio is not small compared to unity, several of the simplifying assumptions employed in Chapter II are not valid for this particular case. If the effect of hysteresis is to be considered, L_m is no longer a real quantity and the value of T_m computed above must be multiplied by the ratio, $1.973/(1 + 0.973/\underline{10°})$, giving

$$T_m \approx 0.09/\underline{-5°} \quad .$$

Also

$$Q = \frac{1 + 0.973/\underline{10°}}{1 + 0.973N_{10}/\underline{\theta_{10} + 10°}} = \frac{1.965/\underline{5°}}{1 + 0.973N_{10}/\underline{\theta_{10} + 10°}} \quad .$$

The leakage factor, k, for the test magnet was not calculable, but it may be assumed to be about 0.05.

For the above parameters the normalized admittance of the test magnet is

$$Y'_m = \frac{1}{1 + j\omega(0.09)/\underline{-5°}\ (0.05 + Q)} \quad ,$$

and the normalized transfer function is

$$G' = Q = \frac{1.965/\underline{5°}}{1 + 0.973N_{10}/\underline{\theta_{10} + 10°}} \quad .$$

These functions are plotted in Figures 15 and 16 along with the experimental data.

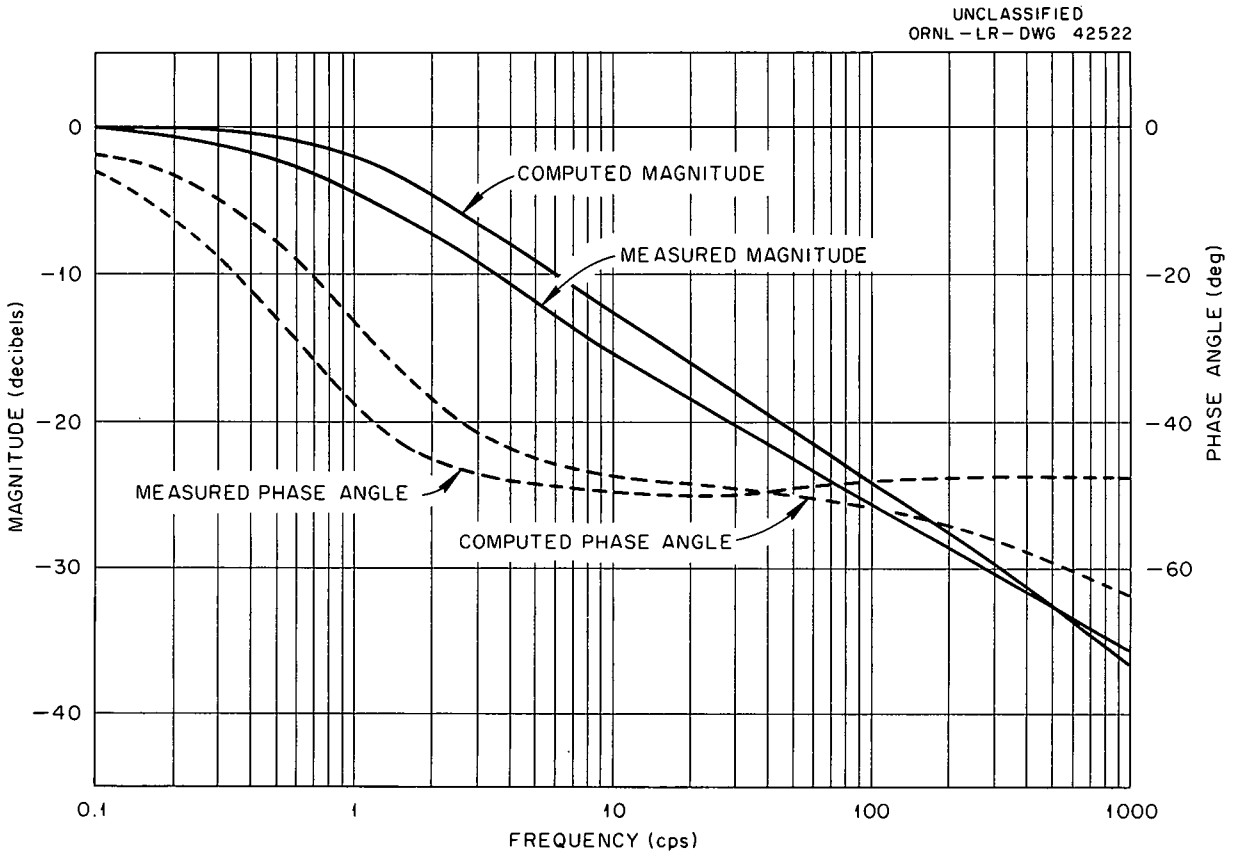

Figure 15. Normalized Admittance (Computed and Measured) of Test Magnet.

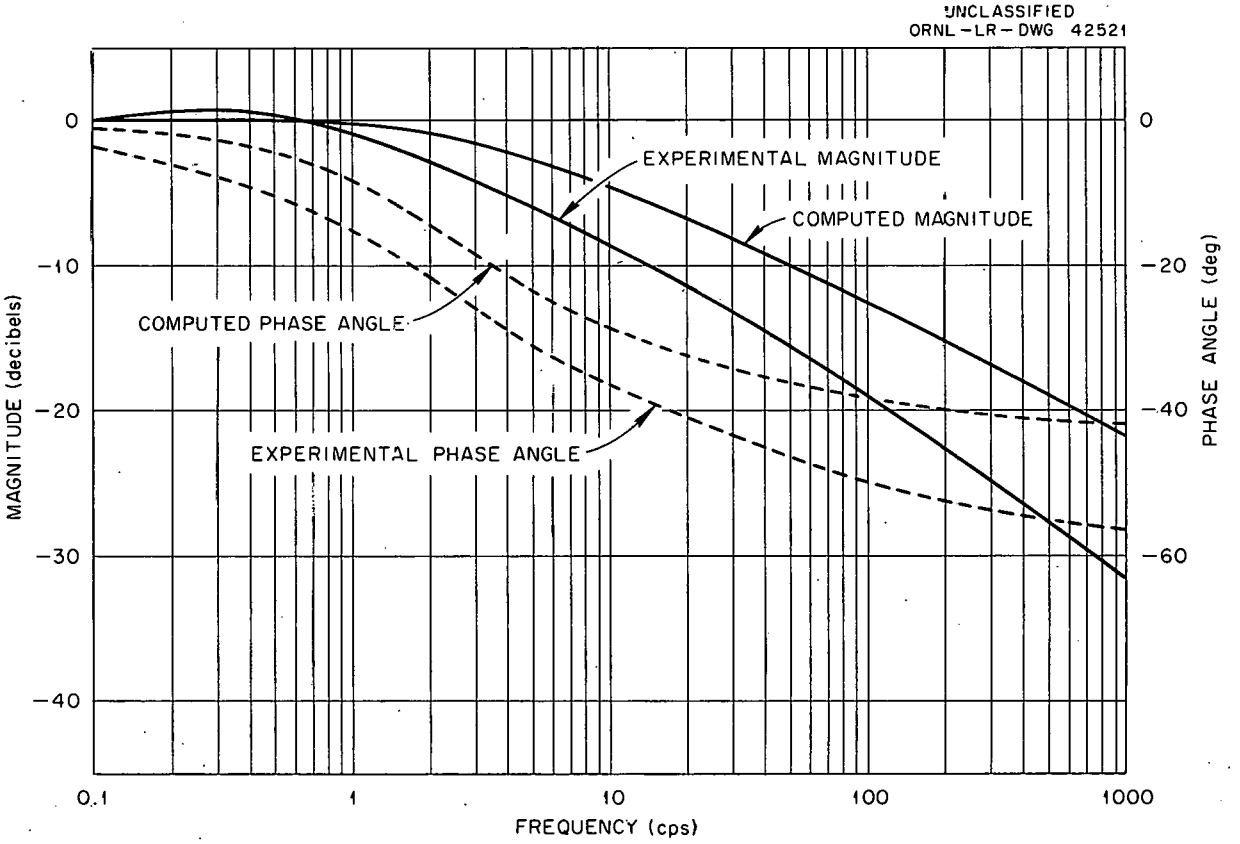

Figure 16. Normalized Transfer Function of Test Magnet.

A block diagram of the measuring equipment is shown in Figure 17. In measuring the admittance and transfer functions the voltage applied to the magnet winding was maintained very nearly constant at $(1.6 + 0.8 \sin \omega t)$. This voltage was also applied to the horizontal amplifier of the oscilloscope, and the a-c component was monitored with a low-frequency, peak-to-peak voltmeter. In measuring the admittance the voltage across a four-ohm resistor in series with the magnet winding was applied to the vertical amplifier of the oscilloscope. Both the amplitude and phase of the magnet current relative to magnet voltage could then be obtained from the resulting Lissajous

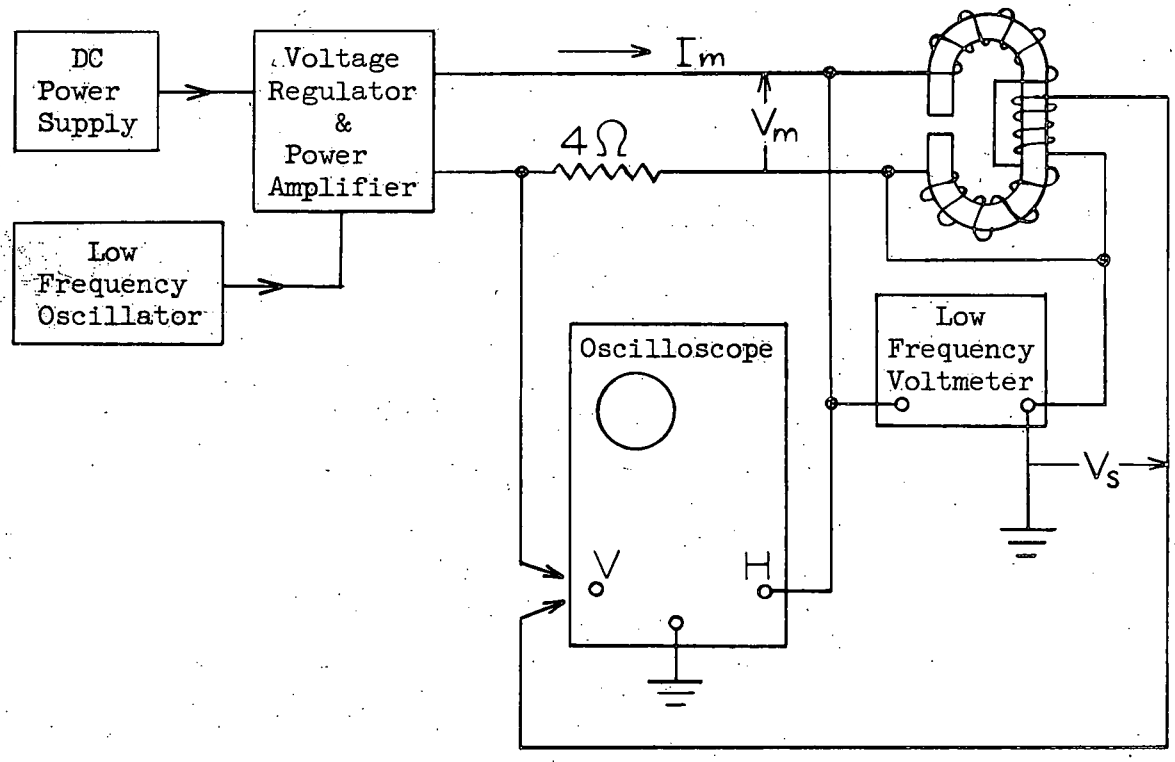

Figure 17. Block Diagram of Measuring Equipment.

pattern. The transfer function cannot be measured directly; however it may be computed if a plot of the induced voltage (as a function of frequency) in a secondary winding is obtained. If V_s = induced voltage in the secondary winding,

$$V_s = N_s \frac{d\phi}{dt}$$

or for sinusoids

$$V_s = j\omega N_s \phi = j\omega N_s A_g B_g.$$

If a plot of V_s/V_m is obtained from Lissajous patterns, then

$$V_s/V_m = j\omega N_s A_g B_g/V_m$$

and

$$G = \frac{B_g}{I_m} = \frac{B_g/V_m}{I_m/V_m} = \frac{1}{j\omega} \frac{1}{N_s A_g} \frac{V_s/V_m}{I_m/V_m}$$

Since the admittance function (I_m/V_m) had been measured, it was relatively easy to obtain G. However, considerable difficulty was encountered in measuring V_s/V_m due to a large amount of noise pick-up (primarily 60 cps) by the secondary coil.

The agreement between the measured and computed admittance functions in Figure 15 is fairly good; however it appears that the value of k assumed (0.05) was too large. If k had been assumed smaller the computed phase would not decrease so rapidly at the high frequency end of the curve. There is also a strong possibility of measurement error at the high frequency end since the signal-to-noise ratio decreases with frequency. The magnet time constant, T_m, appears to be different for the measured and computed case also. This discrepancy may have been due to the relatively large variations employed in the measurements.

The peak-to-peak variation in magnet current for the hysteresis loop in Figure 14, from which L_m was computed, was 0.108 ampere. In measuring the admittance the variation was about 0.4 amp, peak-to-peak, at low frequencies. Since the incremental permeability increases as ΔB increases (over a limited range)[6], the apparent inductance for the measurements may very well have been larger than that calculated from the hysteresis loop. Ideally, the measurements should have been made using a very small variation, but the problem then arises of measuring a small signal in the presence of noise.

The correlation between the computed and observed transfer functions in Figure 16 is rather poor; however, as stated previously, a large amount of noise was encountered in measuring V_s/V_m which increased the probable error in the measurement. Two other factors may also have contributed to the observed error. First, the ratio of iron reluctance to air-gap reluctance may have been in error due to an error in calculating the equivalent air-gap area. Second, an error may arise due to the non-uniform distribution of flux in the air gap since the theory was predicated on a uniform distribution; however this error is undoubtedly small since the flux distribution in the iron should follow Equation 7 very closely except for a small region near the pole tips. The incremental permeability has very little effect on the transfer function for the test magnet. If Q is replotted for $\mu_r = 548$ rather than 274 there is little, if any, change in the magnitude of Q.

Most of the discrepancies between computed and observed data

for the test magnet are a result of the relatively large air gap. In most practical magnets the air gap-to-pole diameter ratio will be much less than that of the test magnet, and calculations should be considerably more accurate.

Although eddy currents external to the iron have received little attention thus far, their effect on the magnet dynamics can be even greater than that of internal eddy currents. This is illustrated in Figure 18 by a plot of the admittance of the 63-inch cyclotron analyzing magnet. As shown in Chapter II, the effect of eddy current coupling in "shorted turns" is easily calculable and the results are quite accurate. The computed time constants for the analyzing magnet were $T_m \approx 1.5$ sec and $T_s \approx 0.5$ second.

The ω_E calculated for the analyzing magnet is 14.5 radian per second. However, there appears to be no noticeable effect on the admittance, due to internal eddy currents. From a qualitative viewpoint this is reasonable since any alternating mmf produced by the magnet winding is opposed by the mmf due to the external eddy currents, and the net alternating mmf acting on the iron core is very small. Of course, if ω_E were less, than, or nearly equal to, $1/T_s$ ($T_s = 0.5$ sec) then the internal eddy currents would undoubtedly affect the admittance.

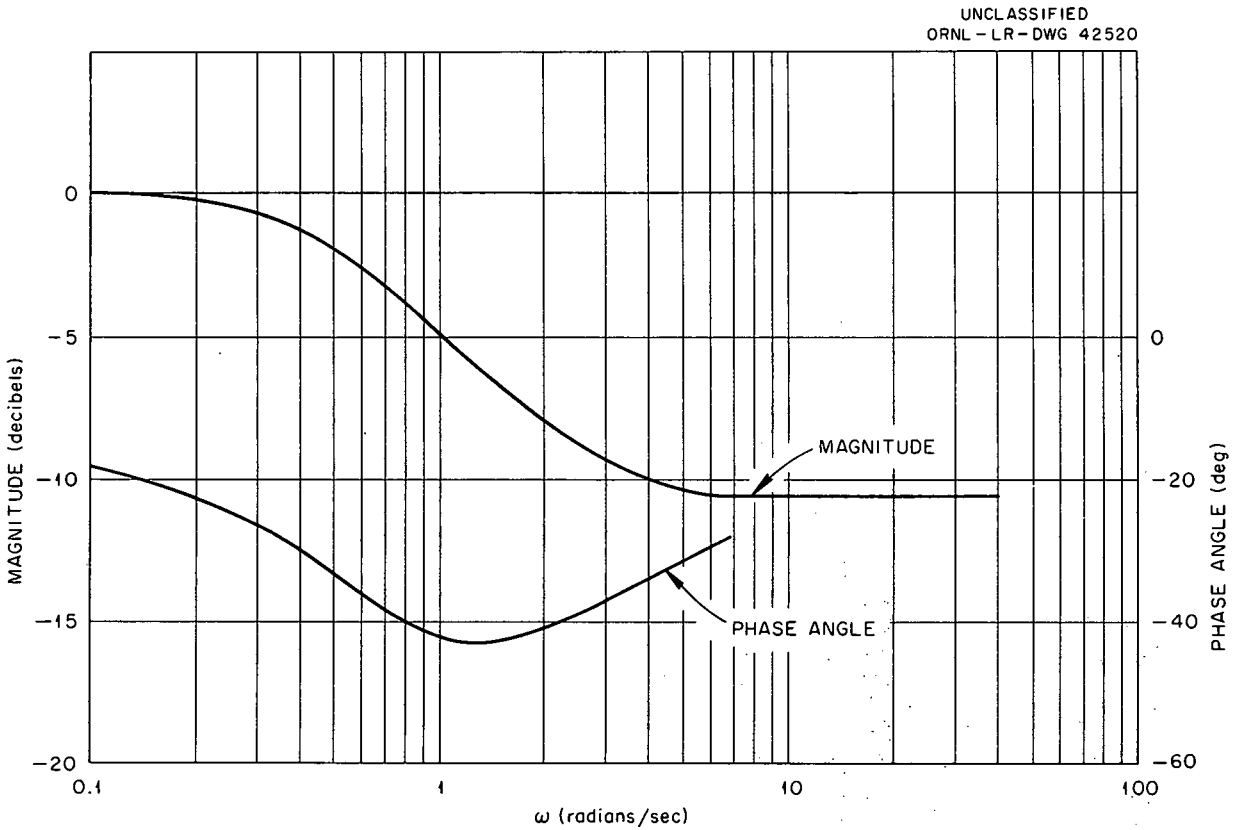

Figure 18. Normalized Input Admittance of an Analyzing Magnet.

CHAPTER IV

CONCLUSIONS AND RECOMMENDATIONS

Although the transfer functions and admittances developed in Chapter II are of some interest academically, their practical importance is in their effect on the magnet control system. To illustrate this effect, a control system will be considered for the magnet assumed in Chapter II.

A block diagram of a typical current regulator is sketched in Figure 19 in which only the primary feedback loop is shown (G_1 may also be stabilized by feedback). It is assumed that the system was designed

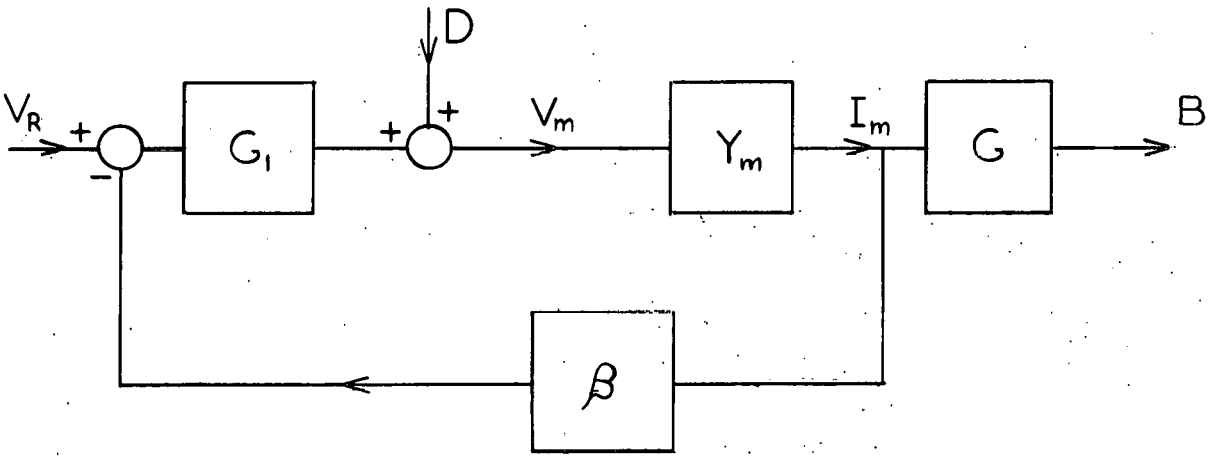

Figure 19. Block Diagram of Current Regulator.

for a magnet in which eddy currents were neglected. From the example in Chapter II

$$\left.\begin{aligned} Y_m &= \frac{1}{1 + j2\omega} \\ G &= K_m \end{aligned}\right\} \quad \text{if eddy currents are neglected.}$$

$$\text{If } G_1\beta = \frac{2(1 + j2\omega)}{j\omega\left[1 + j0.12\omega + (j\omega/5)^2\right]}$$

$$\text{then} \quad G_1 Y_m \beta = \frac{2}{j\omega\left[1 + j0.12\omega + (j\omega/5)^2\right]} \; .$$

This open loop transfer function is plotted in Figure 20 along with the resulting closed loop function. The system is, of course, stable; however if the magnet admittance were actually

$$Y_m = \frac{1}{1 + j1.9\omega(0.05 + Q)}$$

$$\text{where } Q = \frac{1}{1 + 0.05\sqrt{1 + j785\omega}} \; ,$$

then the open-loop transfer function becomes that shown in Figure 21, and the closed loop system would be unstable. Thus it appears that, in certain cases, neglect of eddy current coupling may result in an unstable system. However, if the above system were constructed and found to be unstable, it could be stabilized rather easily by reducing the loop gain by six decibels. The closed loop transfer function for this case is also shown in Figure 21. The reduced gain will, of course, also reduce the regulation attained by the system. A comparison of the regulation achieved in the design case (no eddy currents) and the actual case (eddy currents and reduced gain) may be obtained by considering the effect of the disturbance, D in Figure 19, on the magnetic field. It can be shown that

$$\frac{B}{D} = \frac{1}{G_1\beta} \frac{G_1 Y_m \beta}{1 + G_1 Y_m \beta} \; G.$$

The normalized disturbance transfer functions for the design case and actual case are plotted in Figure 22. The regulation for the design case

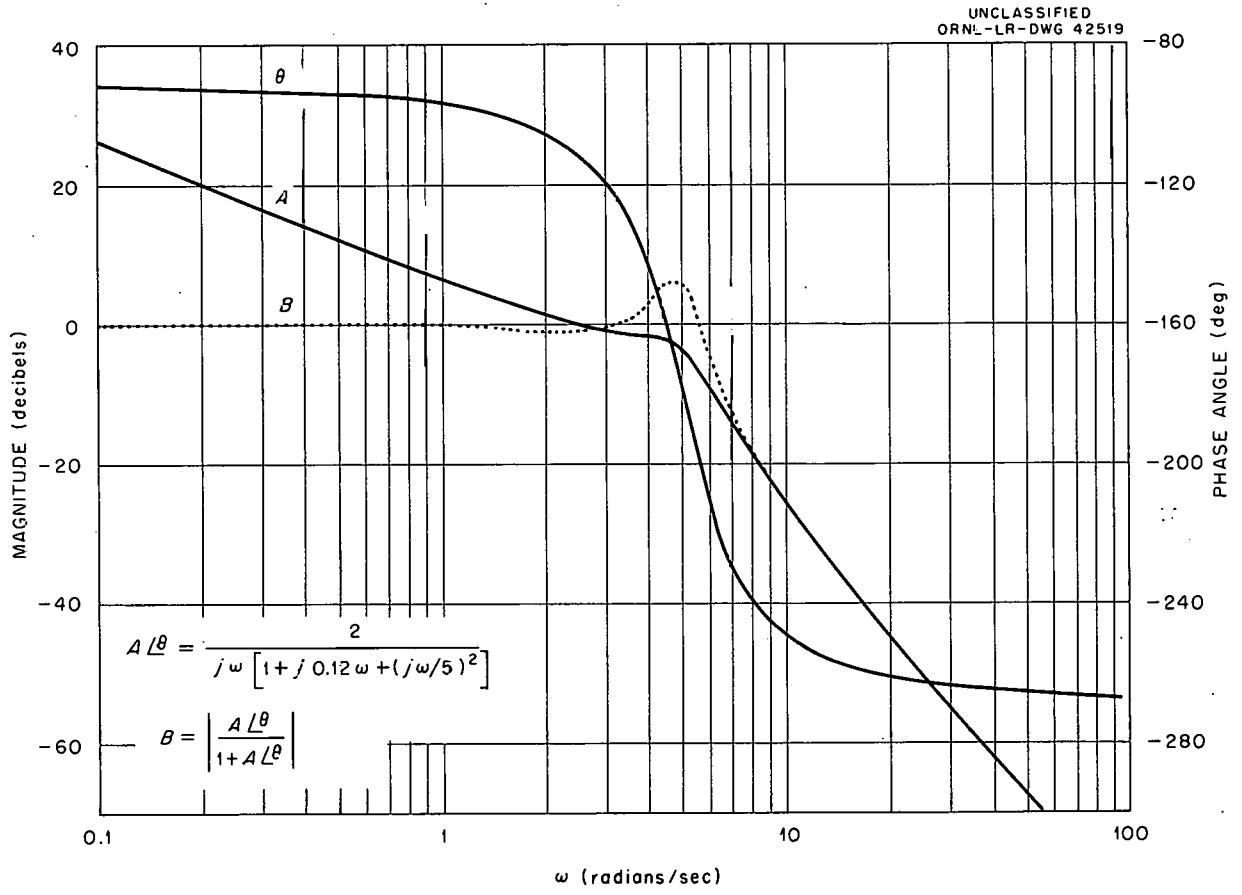

Figure 20. Open- and Closed-Loop Transfer Functions for Assumed Current Regulator.

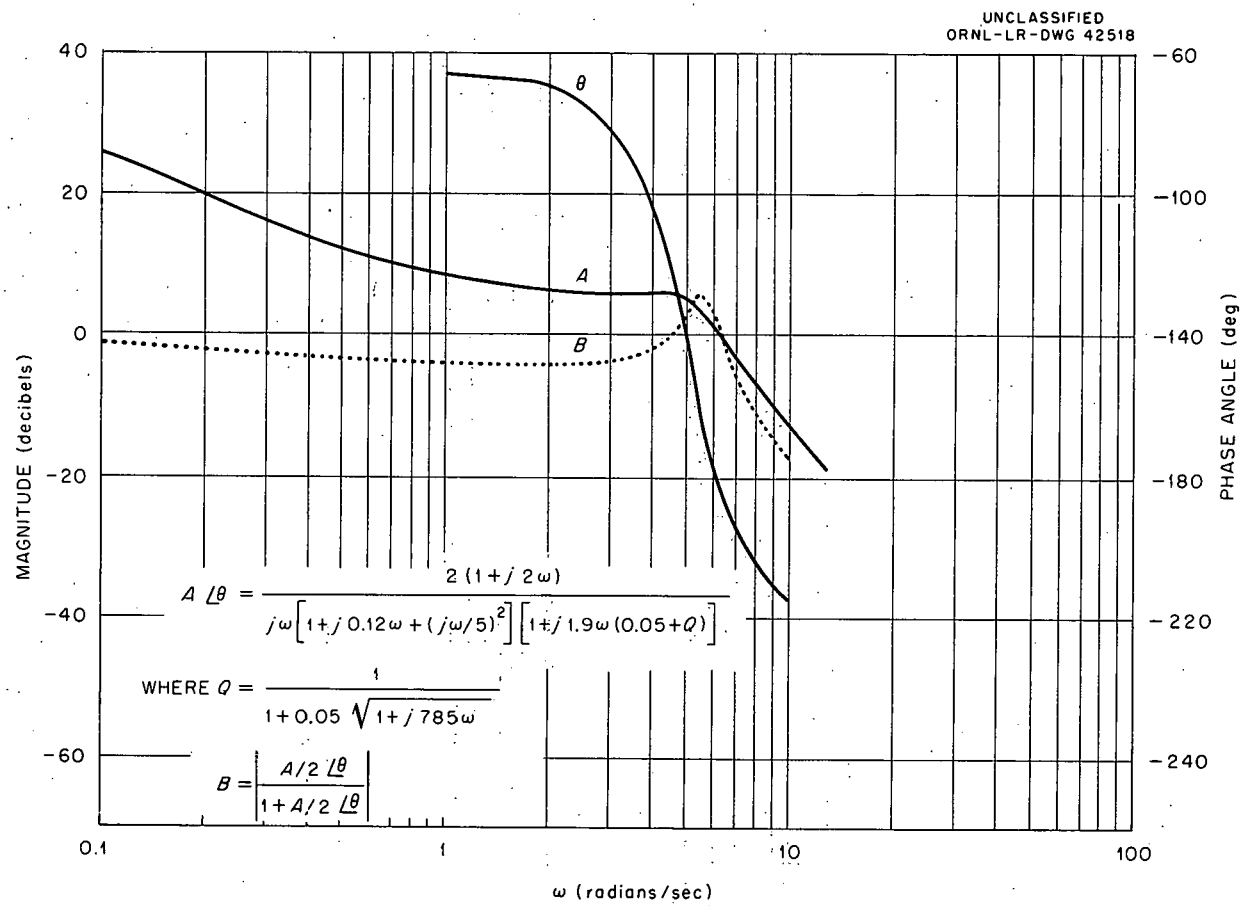

Figure 21. Open- and Closed-Loop Transfer Functions for System with Eddy Current Coupling in Magnet.

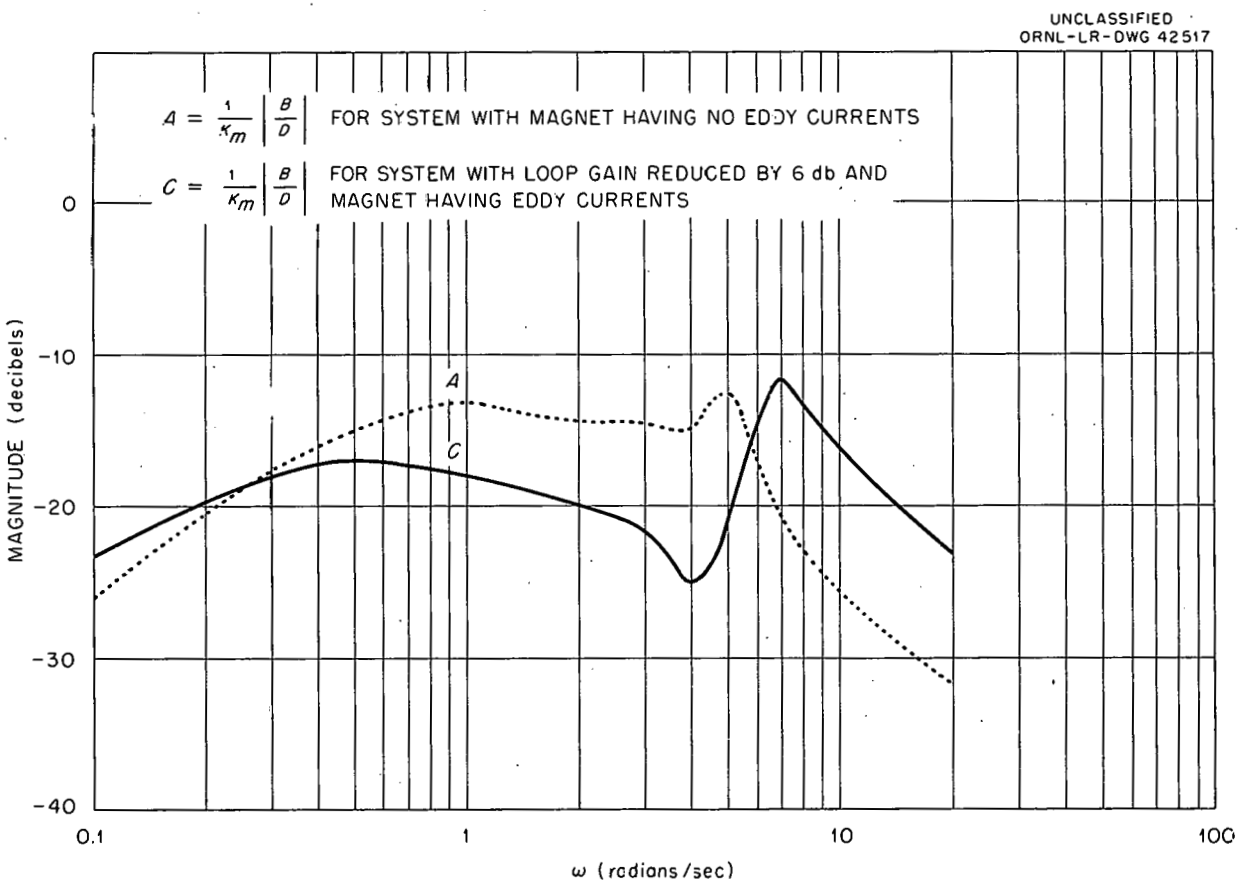

Figure 22. Disturbance Transfer Functions for Two Cases.

is considerably better than that of the actual case except in the range $0.2 < \omega < 6$. The improved regulation over this range is due to attenuation of the magnet transfer function since, for the actual case

$$G \approx \frac{K_m}{1 + 0.05\sqrt{1 + j785\omega}}$$

The actual regulation attained would, of course, depend on the character of the disturbance, D, but if D is a random variation ("white noise"), then the actual system would have considerably poorer regulation than was intended during the design. If the effect of eddy current coupling in the magnet had been considered in synthesizing the above assumed system then a greatly improved regulator could have been designed.

External eddy currents in a magnet assembly may also produce instability and poor regulation if neglected in designing the magnet control system.

One of the most useful stabilizing networks in the design of magnet regulators is the "lead" network. If the magnet admittance is assumed to be $1/(1 + j\omega T_m)$, then the lead network required in the loop has the form $(1 + j\omega T_m)/(1 + j\omega a T_m)$ where $a < 1$. In general, such a network allows the loop gain to be increased with a resulting improvement in regulation. For the system containing a magnet in which only external eddy currents are of importance, the stabilizing network is again quite simple. If the magnet admittance is assumed to be that in Equation 4 then the network should have a transfer function of $\left[1 + j\omega(T_m + T_s)\right]/(1 + j\omega T_s)$. If the internal eddy currents produce a marked effect on the magnet admittance, the stabilizing network required in the loop is no longer as simple as

the preceding one. In general the required network will have a transfer function of the form

$$\frac{(1 + j\omega T_1)(1 + j\omega T_3)(1 + j\omega T_5) \ . \ . \ .}{(1 + j\omega T_2)(1 + j\omega T_4)(1 + j\omega T_6) \ . \ . \ .}$$

where $T_1 > T_2 > T_3 \ . \ . \ .$ The number of factors required in the numerator and denominator will depend upon the frequency range over which the network is to be effective and the rate of attenuation required.

This paper has been concerned exclusively with the frequency response of magnets and regulators; however if the transient response is desired it may be approximated by Floyd's method[7], or for a more exact treatment of the transient response of magnets, the reader is referred to Wagner's paper[2].

In conclusion the effects of eddy currents and hysteresis on the dynamics of a magnet may be summarized as follows:

External eddy currents produce a zero and a second pole in the magnet admittance and attenuate the effect of rapid variations of magnet current on the magnetic field. The effect of external eddy currents may be obscured by internal eddy currents, and vice versa depending on the relative time constants.

Hysteresis has a rather minor effect on magnet dynamics. It primarily affects the phase angle of the magnet admittance and transfer function.

Internal eddy currents tend to produce an attenuation rate of 10 db per decade for the magnet admittance and transfer function. Their

effect may be obscured by either external eddy currents or by large leakage inductance.

Although the admittance and transfer functions developed here are, at best, approximations, they should enable the designer of magnet regulators to predict more accurately the characteristics of the magnet to be controlled prior to its construction and testing.

REFERENCES

1. "EDDY-CURRENTS IN SOLID CYLINDRICAL CORES HAVING NON-UNIFORM PERMEABILITY," HAROLD ASPDEN. Journal of Applied Physics, vol. 23, 1952, pp. 523-528.

2. "TRANSIENTS IN MAGNETIC SYSTEMS," C. F. WAGNER. AIEE Transactions, vol. 50, 1934, pp. 418-425.

3. "BESSEL FUNCTIONS FOR ENGINEERS" (book), N. W. MCLACHLAN. Oxford University Press, London, 1955.

4. "VECTOR PERMEABILITY," K. A. MACFADYEN. Journal of the Institute of Electrical Engineers, vol. 94-III, 1947, pp. 407-414.

5. "THE APPLICATION OF THE FREQUENCY-RESPONSE METHOD TO ELECTRICAL MACHINES," S. K. SEN AND B. ADKINS. Proc. of the Inst. of Elect. Engrs., vol. 103C, 1956, pp. 378-391.

6. "ELECTROMAGNETIC DEVICES" (book), H. C. ROTERS. John Wiley and Sons, New York, 1941.

7. "PRINCIPLES OF SERVOMECHANISMS" (book), G. S. BROWN AND D. P. CAMPBELL. John Wiley and Sons, New York, 1948.

THIS PAGE

WAS INTENTIONALLY

LEFT BLANK

ORNL-2860
Particle Accelerators and
High-Voltage Machines
TID-4500 (15th ed.)

INTERNAL DISTRIBUTION

1. C. E. Center
2. Biology Library
3. Health Physics Library
4-5. Central Research Library
6. Reactor Experimental Engineering Library
7-26. Laboratory Records Department
27. Laboratory Records, ORNL R.C.
28. A. M. Weinberg
29. L. B. Emlet (K-25)
30. J. P. Murray (Y-12)
31. J. A. Swartout
32. E. H. Taylor
33. E. D. Shipley
34. S. C. Lind
35. M. L. Nelson
36. W. H. Jordan
37. C. P. Keim
38. R. S. Livingston
39. F. L. Culler
40. A. H. Snell
41. A. Hollaender
42. M. T. Kelley
43. G. E. Boyd
44. A. S. Householder
45. C. S. Harrill
46. C. E. Winters
47. K. Z. Morgan
48. T. A. Lincoln
49. H. E. Seagren
50. D. Phillips
51. R. J. Jones
52. C. D. Goodman
53. F. T. Howard
54. J. A. Martin
55. A. Zucker
56. J. A. Lane
57. M. J. Skinner
58. R. A. Charpie
59. P. M. Reyling
60. G. C. Williams
61-75. N. J. Ziegler
76. R. F. Christy (consultant)
77. W. A. Fowler (consultant)
78. H. Feshbach (consultant)
79. M. Goldhaber (consultant)
80. M. S. Livingston (consultant)
81. N. F. Ramsey (consultant)
82. J. R. Richardson (consultant)
83. J. A. Wheeler (consultant)
84. J. H. Van Vleck (consultant)
85. ORNL - Y-12 Technical Library, Document Reference Section

EXTERNAL DISTRIBUTION

86. Division of Research and Development, AEC, ORO
87-612. Given distribution as shown in TID-4500 (15th ed.) under Particle Accelerators and High-Voltage Machines category (75 copies - OTS)